Functionalized carbon dots from natural precursors for environmental remediation and renewable energy technologies

Habtamu F Etefa*, Francis B. Dejene
(*Department of Physics*, *Walter Sisulu University*, *Mthatha* 5117, *Eastern Cape*, *South Africa*)

Abstract: The green synthesis of functionalized carbon dots (C-dots) from natural precursors is reviewed, providing a sustainable and versatile platform for environmental remediation and renewable energy technologies. The focus is on methods such as hydrothermal, microwave-assisted, pyrolytic, solvent-based, and ultrasonic routes, with an emphasis on biomass-derived precursors and green solvents. Strategies are given for surface passivation, hybridization, and composite formation to tailor their optical properties and their applications in sustainable technologies are examined. In environmental remediation, they act as efficient photocatalysts for degrading organic pollutants and reducing carbon dioxide (CO_2). For renewable energy, they improve light-harvesting in solar cells and dye-sensitized solar cells. Their notable stability and efficiency are highlighted, alongside persistent challenges in controlling their size, uniformity, and scalability of quantum yield. Future work must clarify the structure-activity relationships for multifunctional compounds, facilitating commercial deployment.

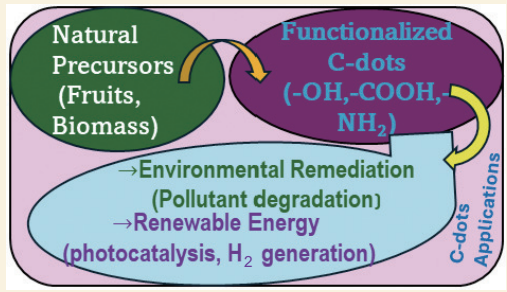

Key words: Carbon dots; Renewable energy; Energy conversion; Natural resource

1 Introduction

Global environmental crises[1], including polluting, green house gas accumulation, and the pressing need for clean energy[2], have catalyzed the search for sustainable and high-performance nanomaterials[3]. In this context, carbon dots (C-dots) have risen as a prime candidate[4], distinguished by their excellent photoluminescence, high aqueous solubility, tunable electronic properties, and facility surface functionalization[5]. The synthesis of C-dots from biomass such as agricultural waste[6–7], lignocellulosic residues, and other natural precursors embodies green chemistry principles[8], transforming abundant, low-value resources into functional nanostructures with a minimal environmental footprint[9–10]. This approach not only addresses waste valorization but also offers a sustainable pathway for nanomaterial production, as highly lighted in recent reviews on circular economy-driven synthesis[11].

Functionalization of biomass-derived C-dots[12–13] opens a gateway to modify their characteristics and develop target-specific applications[6,14–15], which is important. This contribution highlights the latest developments in green synthesis and modification of C-dots with a particular focus on their environmental applications regarding the mechanism of action and efficiency for environmental cleaning by means of photocatalytic dye degradation[16] and heavy-metal sensing[17–18]. Furthermore, it delves into their burgeoning potential in the renewable energy sector, in including applications in hydrogen evolution reaction (HER), CO_2 reduction[19], and as components in supercapacitors and dye-sensitized solar cells (DSSCs)[20–21]. By critically assessing current synthesis bottlenecks, performance limitations, and scalability challenges, this work aims to provide a forward-looking perspective on bridging laboratory-scale innovation with in dustrial-scale application[19, 21-22].

Received: October 20, 2025
Revised: January 04, 2026
Accepted: January 04, 2026

2 Green synthesis of biomass-derived carbon dots: experimental and theoretical advances

Biomass-derived carbon dots (B-CDs, also called carbon quantum dots, CQDs) are now a mature and fast-growing subfield of luminescent nanocarbon research[23]. Over the last 3 years the literature has moved from demonstrations of proof-of concept syntheses (fruit peels, agro-waste) to systematic studies of process, structure and property that connect stock feed chemistry, green processing (hydrothermal microwave, pyrolysis, ultrasonic and solvent-based) and purposeful heteroatom function alization with optical performance, photocatalytic activity and device integration[2].

2.1 Plant-based sources

2.1.1 Experimental outputs: fruits, peels and leaves

Plant juices, fruit pericarps and peel powders are converted to water-dispersible CDs commonly by (1) hydrothermal/solvothermal carbonization (sealed autoclave, 140–220 °C, 2–12 h), (2) microwave-assisted one-pot carbonization (minutes to tens of minutes at 600–1200 W), and (3) simple pyrolysis followed by acid/water extraction and dialysis[24–25]. Hydrothermal and microwave methods dominate because they are solvent efficient, low energy and easily scalable. These protocols produce quasi-spherical nanoparticles (1–10 nm) with abundant oxygen and nitrogen-containing surface groups[26]. Black mulberry (Morus nigra) recent literature reports that the hydrothermal synthesis from black mulberry extract (fruit juice) at ~ 180–200 °C for 6–8 h; resulting C-dots show blue/green emission, good aqueous stabilization and measurable photocatalytic activity for dye degradation under visible light[27]. Reported studies emphasize surface rich functional groups (—OH, —COOH, C=O) as active centers for photogenerated charge separation[28]. Orange peel/orange pomace. Microwave or hydrothermal treatment of orange peel produces CQDs with reported fluorescence quantum yields (QYs) ranging from ~ 10% to over 50%, depending on the solvent, passivation, and removal of larger graphitic fragments. For example, an orange-pomace CQD study reported a QY ≈ 54.3% and excellent photostability when purified and surface-passedivated; other orange peel syntheses report QYs in the 10%–30% range using simpler treat ments. Applications demonstrated include metal-ion sensing, bioimaging and food-safety sensing (Fig. 1)[29].

Natural precursors of C-dots offer sustainable, cost-effective, and eco-friendly alternatives to synthetic chemicals. Here we discuss major synthesis methods with detailed comparisons.

In Table 1, it is clear that hydrothermal methods are the most common for achieving balanced proper-

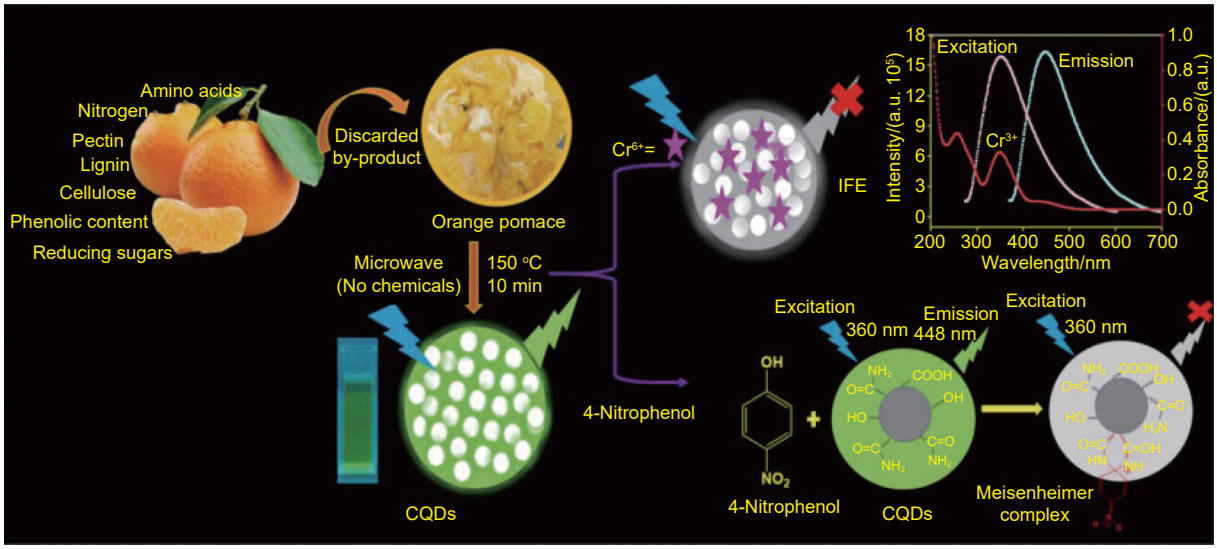

Fig. 1 Orange peel extracted[29]. Copyright 2023, American Chemical Society

Table 1 Bioderived precursor synthesis of carbon dots

Precursor	Temperature/°C	Time/h	Size/nm	Shape	Surface area/(m^2/g)	Yield/%	Application	Ref.
Hydrothermal synthesis from natural precursors								
Orange juice	180	12	2–6	Spherical	~ 45	18–22	Fe^{3+} sensing, bioimaging	[30]
Banana peel	200	5	3–8	Quasi-spherical	~ 52	15–20	Antibacterial, photocatalysis	[31]
Egg shell membrane	200	10	2–5	Spherical	~ 60	12–15	Cr(VI) detection, cell imaging	[32]
Aloe vera	180	8	3–7	Spherical	~ 48	20–25	Drug delivery, bioimaging	[33]
Coffee grounds	220	6	4–9	Spherical	~ 55	10–14	LED fabrication, sensing	[34]
Microwave synthesis from natural precursors								
Garlic	160	10	2–5	Spherical	~ 40	25–30	Antioxidant, bioimaging	[35]
Honey	140	20	2–4	Spherical	~ 38	30–35	Biocompatible imaging probes	[36]
Sugarcane juice	170	12	2–5	Spherical	~ 41	22–28	Anticancer drug carrier	[37]
Carrot juice	180	8	3–7	Quasi-spherical	~ 45	20–25	Metal ion sensing	[38]
Pyrolysis from natural precursors								
Soybean	300	2	4–10	Irregular	~ 65	35–40	Bioimaging, sensor	[39]
Grass	350	1.5	5–12	Spherical	~ 70	30–35	Photocatalysis	[40]
Egg	280	2.5	4–9	Spherical	~ 62	28–33	Fluorescent ink, sensor	[41]
Solvent-based synthesis from natural precursors								
Cinnamon	Water/Ethanol	120	6	2–6	Spherical	15–20	Antioxidant, anti-inflammatory	[42]
Tulsi leaves	Water	100	8	3–7	Quasi-spherical	12–18	Anticancer, bioimaging	[37]
Potato peels	Ethanol	110	5	4–9	Spherical	10–15	Heavy metal detection	[43]
Turmeric	Ethanol	90	10	2–5	Spherical	18–22	Cellular imaging, drug delivery	[44]
Ultrasonic synthesis from natural precursors								
Lemon peel	30	45	2–5	Spherical	8–12	pH sensing, bioimaging	Lemon peel	[45]
Papaya	40	60	3–6	Spherical	10–15	Antioxidant, metal ion sensing	Papaya	[46]
Tea leaves	50	30	3–7	Quasi-spherical	12–16	Fe^{3+} detection	Tea leaves	[47]

ties. Microwave synthesis offers speed, whereas pyrolysis yields large yield. Solvent-based methods typically allow for greater control over chemical tuning. Ultrasonic methods are energy-efficient.

As revealed in Table 2, solvent usage is strongly protocol dependent. Hydrothermal syntheses are typically aqueous but use large water dilutions. Microwave methods are often run at higher concentration, and for shorter times, so the effective L per kg final product tends to be lower. (See Crista 2020 LCA and supporting tables for per-kg inventory)[48]. The ranges above combine direct experimental energy measurements and published LCA conclusions. Where authors gave per-kg LCA inputs (e.g., inputs for producing 1 kg of CDs), those were used to derive per-kg energy/solvent estimates; where only small-batch energy was reported I scaled to kg using the reported yields. See the cited LCA / experimental papers for protocol-level details and the supplementary inventory (e.g., inputs for 1 kg production in Crista et al. 2020)[48].

This comparative Table 2 quantitatively substantiates that microwave-assisted synthesis is a significantly more environmentally efficient green synthesis route for carbon dots (C-dots) than the hydrothermal method across all measured metrics. The microwave

Table 2 Comparison table: hydrothermal vs microwave-assisted method

Method	Measured energy consumption/(kWh·kg^{-1}, CDs)	Solvent usage (typical, L·kg^{-1}, CDs)	Estimated carbon footprint (kg CO_2-eq · kg^{-1} CDs)
Hydrothermal	Reported / reviewed values: ~ 10 – 35 kWh/kg (literature reports up to ~ 35 kWh per 1 kg CDs for some protocols; values vary widely because of low yields and long heating times)[49]	Mostly water (but large dilution): tens → hundreds of L per kg (depends on precursor concentration; hydrothermal studies commonly use mL per g precursor — scales to large L per kg of final product)[50]	~ 8.6 – 30.3 kg CO_2 e/kg using SA grid factor 0.8665 kg CO_2 e/kWh (0.8665 × 10 → 0.8665 × 35). (Replace factor for other[51]
Microwave assisted	Reported / measured values: reported single studies ~ 1–5 kWh/kg (example: 4.33 kWh/kg reported for a microwave N-doped CD study; LCAs and comparative studies consistently show microwave to be much lower energy per kg than hydrothermal)[52]	Usually water or small solvent amounts; overall much lower solvent volumes per kg than hydrothermal because of small reaction volumes and short times (typical lab reports use mL scale but higher yield reduces per-kg solvent)[48]	~ 0.9 – 4.0 kg CO_2e/kg using SA grid factor 0.8665 kgCO_2e/kWh (0.8665 × 1 → 0.8665 × 4.33)[53]

process consumes an order of magnitude less energy (1–5 vs. 10–35 kWh kg^{-1} of C-dots), directly resulting in a proportionally lower carbon footprint (0.9–4.0 vs. 8.6–30.3 kg CO_2-equivalent per kg). Furthermore, due to higher reaction efficiency and yields, microwave synthesis requires substantially less solvent per kilogram of final product, minimizing water usage and waste. Therefore, while both methods utilize green precursors, the microwave route's drastic reduction in process time and energy intensity provides a far superior environmental profile, validating stronger sustainability claims.

2.1.2 Theoretical/mechanistic outputs

The generally accepted multi-step formation mechanism for plant-derived CDs is (1) dehydration and polymerization of soluble biomolecules (sugars, pectins and amino acids), (2) nucleation of conjugated aromatic clusters by aromatization/carbonization, and (3) surface functionalization/passivation by residual bio-molecules or added dopants. The relative abundance of carbohydrates, polyphenols and proteins in the precursor controls the chemical pathways and the degree of graphitization. Recent experimental-theoretical studies provide kinetic/engineering insights into how hemicellulose/cellulose fractions versus polyphenols steer nucleus formation and surface chemistry [54].

As shown in Fig. 2, the schematic illustrates the green conversion of rice husk waste into carbon dots (CDs) by optimised hydrothermal synthesis[55]. Rice husk, produced in massive quantities worldwide (157.5 million tons in 2021), is rich in cellulose, hemicellulose, lignin, extractives, proteins, and ashes, all of which serve as carbon sources. During hydrothermal treatment (149–220 °C, solid load 2.93–17.07 m/v), these biopolymers undergo dehydration, polymerization, and aromatization reactions to generate small conjugated carbonaceous nuclei, which subsequently evolve into nanoscale carbon dots[56–57]. The process converts the molecular building blocks such as glucose units from cellulose, xylose/arabinose from hemicellulose, phenylpropanoids from lignin, amino acids from proteins, and various extractives into fluorescent sp^2/sp^3-hybridized carbon structures with surface functional groups that provide water solubility and tunable photoluminescence. The resulting CDs exhibit strong blue emission under UV light and can be tailored by adjusting synthesis parameters, making

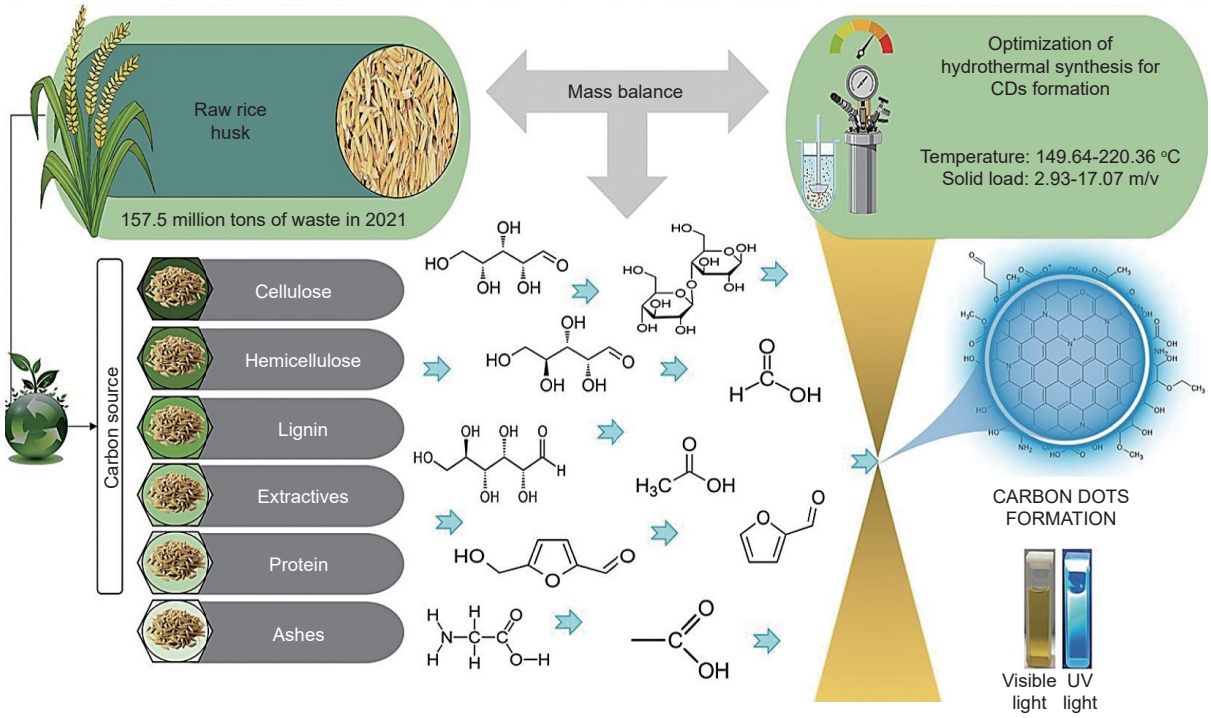

Fig. 2 Mechanism for plant-derived CDs[54]. Copyright 2025, Elsevier

this approach an environmentally friendly valorization route for agricultural waste[57].

2.2 Synthesis methods

Since their discovery, the methods for producing carbon quantum dots (CQDs) have evolved into convenient, low-cost and scalable processes (Fig. 3). These synthesis strategies fall into two main categories: top-down and bottom-up. Despite the relative ease of production, challenges remain in preventing nanomaterial aggregation, controlling size and uniformity, and fine-tuning surface properties. To enhance performance, post-treatment methods can modify surface functional groups. For instance, surface passivation boosts quantum yields by removing emissive traps, while doping with heteroatoms (N, P) or metals (Au, Mg) improves solubility and conductivity. Although both synthetic approaches are used, the bottom-up method is generally favored for its cost-effectiveness and environmental benefits[58].

2.2.1 Hydrothermal/solvothermal carbonization: controlled, tunable, widely used

Mix a carbonaceous precursor (sugars, fruit peels, proteins, citric acid, lignin, etc.) in a solvent (water is most common), seal in an autoclave and heat at elevated temperature and autogenous pressure. Under those conditions the precursor molecules dehydrate, polymerize and aromatize. Nucleation and carbonization produce nano-sized sp^2/sp^3 carbon cores while the solvent and reaction chemistry leave oxygen- and nitrogen-containing surface groups (—COOH, —OH, $—NH_2$) that dominate solubility and surface chemistry[60–61]. Typical condition ranges & tunable knobs: 120–240 °C (many reports use 160–220 °C), reaction times from tens of minutes up to 12–48 h; precursor concentration, pH (strong effect on surface groups and emission), solvent (water vs alcohols), and added dopants (urea, ammonia, thiourea) strongly change size, surface functionality and quantum yield[61]. Higher temp/longer time -> more carbonization (smaller, more graphitic cores) and often bathochromic shifts; pH controls protonation/deprotonation of surface moieties and hence PL and surface charge[62–63].

This method is green (water solvent possible), easy to implement, good control over surface chemistry (important for adsorption/photocatalysis), and adaptable to many biomass wastes. It also scales reasonably (batch scale-up and microreactor/continuous hydrothermal reactors have been demonstrated)[64]. Relatively slow (hours), product often contains a mix-

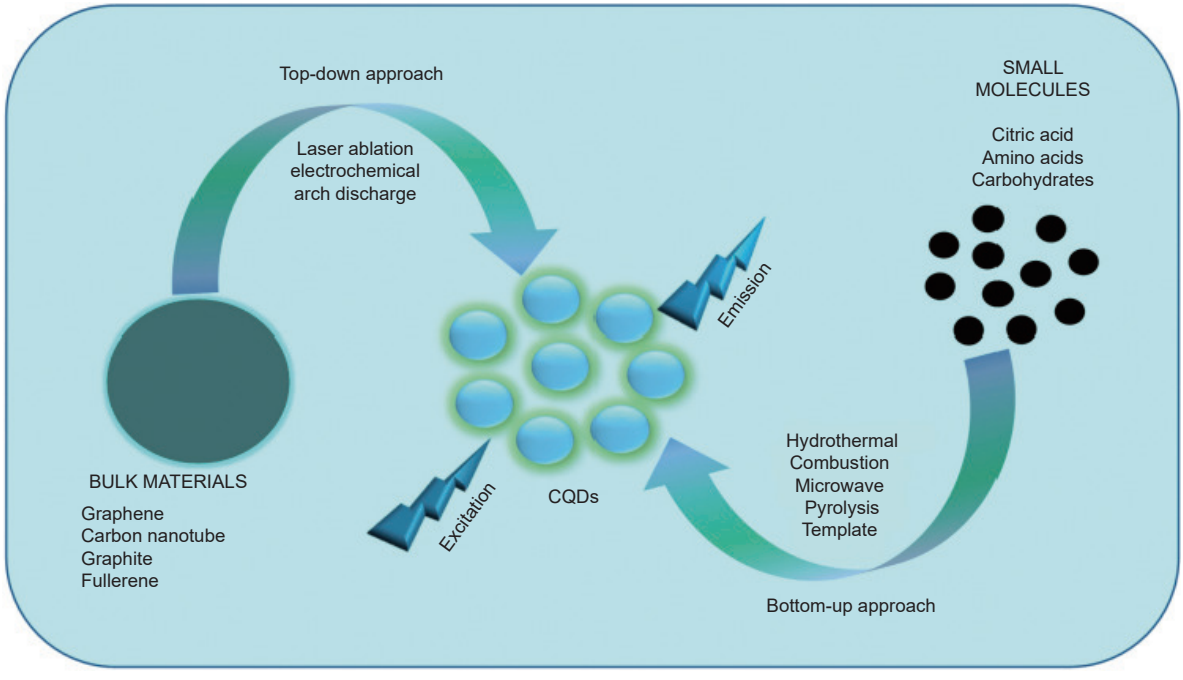

Fig. 3 The typical approaches for the synthesis of CQDs[59]. Copyright 2023, MDPI

ture of small molecules, oligomers, and true nanodots so purification (centrifugation, ultrafiltration, dialysis, column chromatography) is commonly required to isolate narrow size fractions and remove small fluorescent byproducts. Reproducibility between labs can be an issue unless conditions and precursor composition are tightly controlled[65]. Applications where well-defined surface groups matter, e.g., photocatalyst modifiers, pollutant adsorption/photodegradation (surface carboxyls and hydroxyls help binding and charge transfer), biosensing and biological applications where water-compatibility and gentle processing are needed[66].

2.2.2 Microwave-assisted synthesis: ultrafast, energy-efficient, great for doping

Use microwave irradiation (household or lab microwave reactors) to heat the precursor mixture volumetrically[67]. Microwave heating accelerates the dehydration/carbonization/polymerization steps by very fast heating rates (tens to hundreds °C/min); local "hot spots" and rapid kinetics favor quick nucleation and carbon core formation[68]. Heteroatom dopants (N, S, P, B, metals) can be introduced simply by adding small molecules (urea, thiourea, ammonium salts, metal salts) to the precursor mix[69]. Typical condition ranges & outcomes: reaction times of seconds-to-minutes (commonly 1–10 min) at modest bulk temperatures; reported quantum yields can be high when appropriate passivation/doping is used[70]. Because the process is so fast, reaction power, microwave absorption properties of the precursor, and precursor ratios are the critical knobs[71]. Advantages: extremely fast, energy-efficient, often single-step, easy doping for improved electronic/photocatalytic properties, and promising for rapid prototyping or small-scale production. Many studies report good PL and high QY using microwave routes[72–73]. Limitations & cautions: microwave chemistry is sensitive to the exact apparatus (field distribution, cavity, vessel geometry) so reproducibility and scale-up are non-trivial[74]. "Hot-spot" effects can produce broader size distributions unless carefully optimized. Safety note: some precursor/solvent combinations (closed metal vessels, flammable solvents) require proper microwave reactors[75]. Best for: rapid generation of doped CDs for sensor strips, fluorescence-based pollutant detectors, or applications where fast screening of dopants/conditions is valuable[76–77]. With optimization it also yields photoactive doped CDs useful as electron-mediating additives in photocatalysis or as conductive additives in electrodes.

2.2.3 Pyrolysis/combustion/ thermal decomposition: solvent-free, highly scalable, but less uniform

Dry (solid-state) heating of biomass or organic precursors in air-limited or inert atmosphere (pyrolysis) to thermally decompose polymers into carbonaceous residues; at controlled temperatures organic fragments aromatize and nanoscale carbon domains form[78–79]. Combustion/combustion-assisted methods (flame, spontaneous combustion) and solvent-free thermal carbonization are also used for fast, large-scale production. Reported thermal treatments for CDs vary widely: some solvent-free thermal degradations run at ~ 200–300 °C, while conventional pyrolysis for more graphitic chars spans 300–1000 °C depending on desired product[80]. Advantages: simple (often no solvent), low-cost, easily applied to large volumes of waste biomass, and can yield high mass conversion (some reports show high carbon yield at optimized calcination conditions)[81]. Pyrolytic CDs tend to have more conjugated (sp^2) cores useful where conductivity and graphitic domains are needed (e.g., electrode additives, some photocatalytic supports)[2]. Limitations: broader size distributions, more structural heterogeneity, surface functional groups are less abundant (so surface activation/passivation often required), and the product contains large particulates and ash that must be removed. Purification is often more involved; control over PL color and bright QY is harder than with wet bottom-up routes without extra passivation[4]. Best for: large-scale, low-cost production where absolute nanoscale monodispersity is less critical e.g., bulk adsorbents, composite fillers, electrode materials, or when the CD is used as a conductive/photoactive additive rather than as a discrete fluorescent probe.

3 Optical properties of carbon dots

CDs, due to their carbon-based structure, typically absorb ultraviolet (UV) light strongly, with this absorption often extending into the visible range. Their optical profile is generally characterized by a primary absorption peak around 250 nm, resulting from the π–π* transitions of C=C bonds, and a secondary peak between 300–400 nm caused by n–π* transitions of C=O or C=N bonds (Fig. 4a). Some CDs can absorb light across a wider spectrum, even into the visible and near-infrared (vis-NIR) range. For instance, fluorine-doped CDs show specific peaks at 556 and 624 nm, which are linked to C=N bonds in specific nitrogen structures (Fig. 4b). Additional NIR peaks have been attributed to large sp^2 carbon domains connected by strong hydrogen bonds.

A defining and attractive feature of CDs observed, in early studies, is their bright, multi-color fluorescence, which is both stable and easily adjustable. This photoluminescence (PL) occurs when the dots absorb energy and then re-emit it as light. For graphene quantum dots (GQDs) and CQDs, the emission color is heavily dependent on their size due to the quantum confinement effect; larger dots emit redder light, while smaller ones emit bluer light (Fig. 4c).

Furthermore, post-synthesis modifications like surface passivation or functionalization profoundly impact their light-emitting properties. For example, Sun and colleagues used a polymer to passivate CDs,

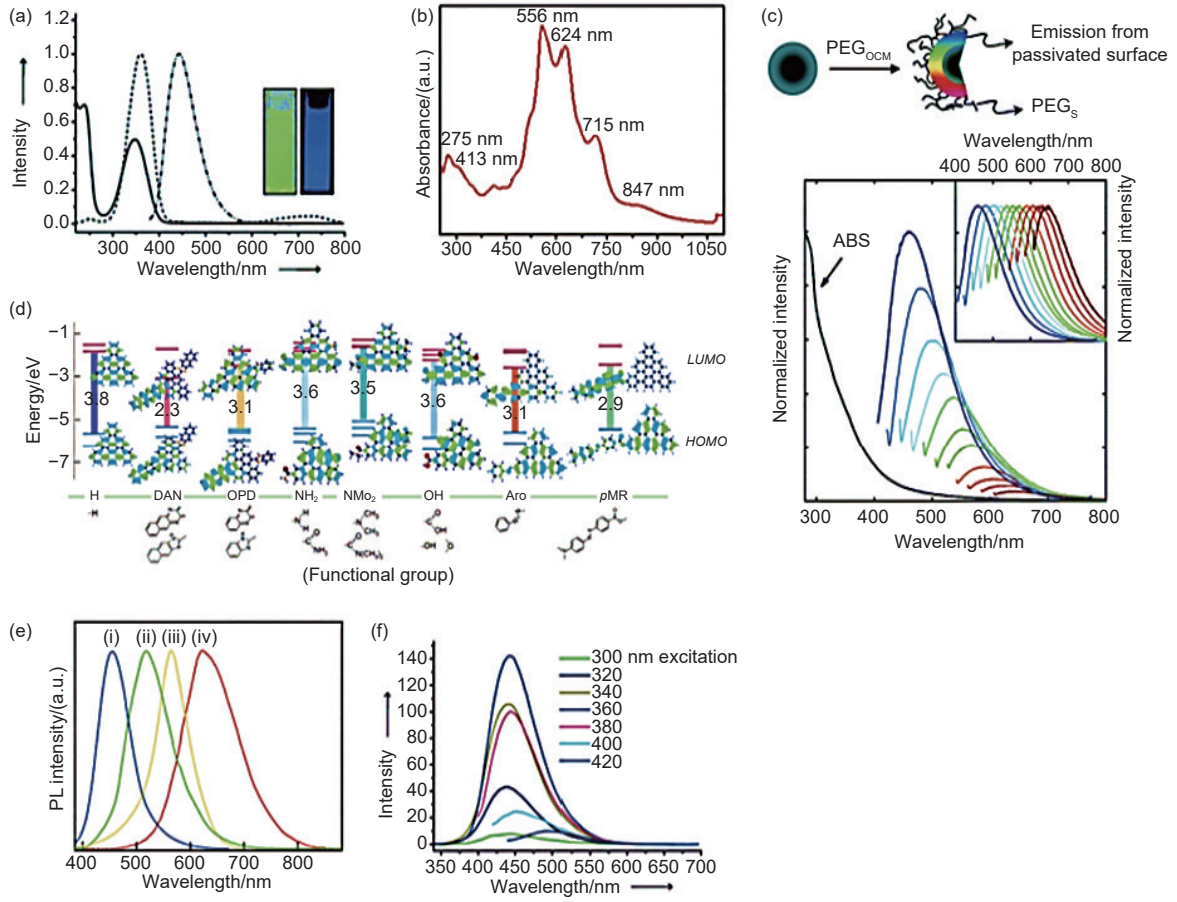

Fig. 4 (a) UV–vis absorption spectra (solid line) of CDs in aqueous solution hydrothermally synthesized from CA and EDA. Reproduced with permission[82]. Copyright 2013, Wiley-VCH. (b) UV–vis absorption spectra of F-doped CDs prepared by solvothermal method. Reproduced with permission[83]. Copyright 2020, Wiley-VCH. (c) Schematic illustration of surface passivation and PL emission spectra of PPEI-EI passivated CDs in an aqueous solution. Reproduced with permission[84]. Copyright 2006, American Chemical Society. (d) Predicted energy level diagrams for GQDs with different nitrogen functional groups. (e) Normalized PL spectra of (i) Azo-GQDs, (ii) NH_2-GQDs, (iii) OPD-GQDs, and (iv) DAN-GQDs from blue to red. Reproduced with permission[85]. Copyright 2016, Wiley-VCH. (f) Excitation dependence of CDs in aqueous solution hydrothermally synthesized from CA and EDA. Reproduced with permission[85]. Copyright 2016, Wiley-VCH

resulting in intensely bright, multi-colored emissions. The researchers explained this was due to the stabilization of surface energy traps. In another case, Tetsuka's team created amino-functionalized GQDs (Fig. 4d). They found that modifying the dots with different amine compounds could raise or lower their energy levels, enabling the production of CDs that emit light across the entire visible spectrum, from blue to red. One of the most intriguing features of CDs lies in their stable, easily tunable, and multicolored fluorescence, which attracted great attention during the early stages of research. PL typically arises from radiative transitions following photon energy absorption. The emission wavelength of GQDs and CQDs is strongly size-dependent due to the quantum confinement effect (QCE), where an increase in particle size leads to a red shift in PL emission, and a decrease results in a blue shift. Furthermore, surface modifications such as passivation or functionalization have a substantial impact on the PL properties. For example, Sun et al. enhanced the bright multicolor fluorescence of CDs synthesized via laser ablation by passivating them with poly(propionylethyleneimine-co-ethyleneimine) (Fig. 4e). This enhancement was attributed to surface energy traps that became emissive after polymer stabilization. Similarly, Tetsuka et al. prepared amino-functionalized GQDs through nucleophilic substitution reactions between amine groups and oxygen-containing functional groups on the GQDs (Fig. 4d). They observed that GQDs modified with primary or dimethyl amine groups exhibited elevated energy levels due to degraded HOMO orbitals, whereas modifications with o-phenylenediamine, diaminonaphthalene, or azo groups resulted in lower energy levels, thereby yielding multicolored luminescent CDs with emissions ranging from blue to red (Fig. 4e). The PLs behavior of carbonized polymer dots (CPDs) differs somewhat from that of CQDs and GQDs. Typically, CPDs exhibit a broad full width at half maximum (FWHM) in their PL spectra, with emissions primarily in the blue or green regions, and they often display strong excitation-dependent fluorescence (Fig. 4f). This distinct behavior arises from the complex polymer/carbon hybrid structure of CPDs, which allows the coexistence of multiple fluorescent centers within a single nanoparticle, leading to varied emission energy levels.

Table 3 summarizes the synthesis of CDs derived from various renewable feedstocks using green solvents. The quantum yield (QY) and particle size of CDs depend strongly on the nature of the precursor and synthesis route. For instance, o-phenylenediamine and wild raw neem bark yield notably high QYs of 98.5% and 36.25%, respectively, while natural precursors such as kiwifruit juice, soybeans, and citric acid produce moderate yields ranging from 2.4% to 16.7%. The particle sizes of CDs vary between 0.66 and 20 nm, reflecting the influence of carbon source composition and processing conditions. These findings highlight that biomass-derived precursors not only serve as sustainable and cost-effective carbon sources but also enable tunable control over the optical and structural properties of CDs through eco-friendly synthesis pathways.

Table 3 Carbon dots synthesis using green solvents

Renewable feedstock	QY of CDs/%	CDs particle size/nm	Ref.
Kiwifruit juice	2.4–10.0	4.8–6.9	[86]
Urea	16.2	3.9	[87]
Soybeans	16.7	1.0-3.0	[88]
Glycine	14.0	4.0–20.0	[89]
Crab shells	14.5	8.0	[90]
Dextrose	-	3.2	[91]
o-phenylenediamine	98.5	0.7–2.7	[92]
Wild raw neem bark	36.3	2.0–10.0	[93]
Vine tea	20.4	2.7	[94]
Sophora flavescens aiton	31.6	2.8	[95]
Citric acid	2.4	3.1	[96]

4 Functionalization strategies of carbon dots

In a study by Chen et al. [97], a fluorescent probe for copper and sulfide ions was created. The team synthesized carbon dots (CDs-5) from citric acid and ethylenediamine (Fig. 5), followed by surface modification with cyclam a molecule known for its strong binding with Cu^{2+}. The mechanism relies on FRET: Cu^{2+} binding quenches the CDs' fluorescence, while

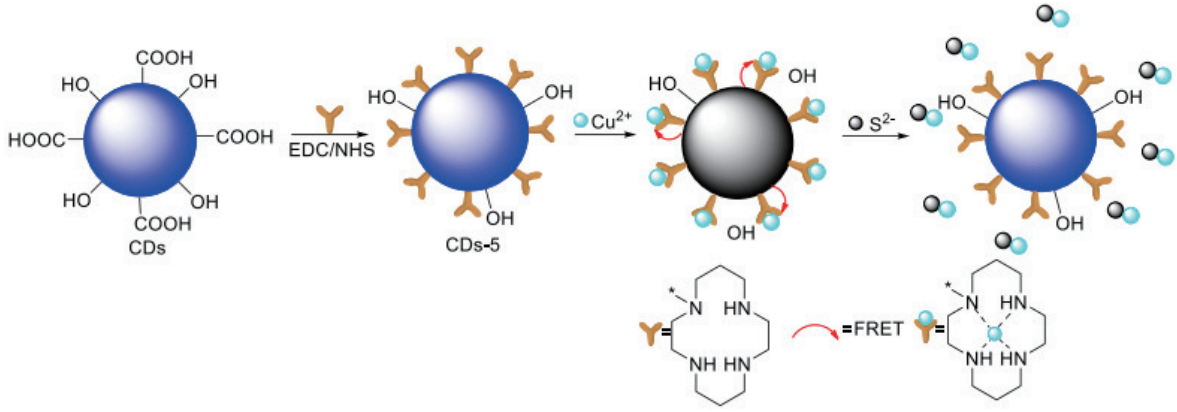

Fig. 5 The synthesis process of CDs-5 via amide coupling reaction and the detection mechanism for Cu^{2+} and S^{2-} [98].
Copyright 2018, Springer-Verlag GmbH Austria, part of Springer Nature

subsequent addition of S^{2-} displaces the copper, restoring the signal due to the higher stability of the formed CuS. This highly sensitive assay (LOD: 0.1 μmol L^{-1} for Cu^{2+}, 0.13 μmol L^{-1}M for S^{2-}) was also non-toxic and effective for monitoring these ions within biological systems, specifically HeLa cells. Fig. 5 illustrates a two-part process centered on specially functionalized CDs-5. First, the CDs are synthesized through an amide coupling reaction, which introduces specific surface groups that act as binding sites. These engineered CDs then serve as a fluorescent sensor for the sequential detection of Cu^{2+} and S^{2-}. The mechanism is based on a fluorescence "on-off-on" response: the initial fluorescence is quenched when Cu^{2+} binds to the CD surface, and the signal is subsequently restored when S^{2-} is introduced, as the sulfide ions selectively remove the bound copper due to their stronger affinity, forming CuS. This design enables a highly specific and reversible detection method for both ions.

4.1 Heteroatom doping

Heteroatom doping is a cornerstone strategy in the engineering of CDs, fundamentally aimed at tailoring their intrinsic electronic structure, surface chemical properties, and ultimately, their functional performance. The incorporation of atoms with different electronegativities and atomic sizes into the carbon lattice (lattice doping) or attached to the surface (surface doping) disrupts the uniform electron density distribution of the sp^2 carbon framework. This perturbation introduces defect states, modulates the bandgap, enhances charge separation/transfer, and creates active sites, leading to significant improvements in properties such as fluorescence quantum yield, catalytic activity, and electrochemical performance.

The efficacy of doping is governed by the dopant's electronegativity (χ) relative to carbon (χ = 2.55). Nitrogen (χ = 3.04), being more electronegative, acts as an electron acceptor, while sulfur (χ = 2.58) and phosphorus (χ = 2.19) can act as electron donors, each creating unique local electronic environments.

4.2 Nitrogen doping

Nitrogen doping (N doping) is the most prevalent and extensively studied doping method for CDs due to its comparable atomic size and the strong valence bonds it can form with carbon (C—N, C=N). The enhancement in properties is primarily attributed to the increase in electron density and the creation of new energy levels within the carbon matrix. The coexistence of N-types creates a heterogeneous electronic environment that facilitates electron-hole pair separation and narrows the bandgap, leading to a red-shift in fluorescence and enhanced photoluminescence quantum yield (PLQY). The electron-rich sites created by N-doping are highly effective for catalytic processes, particularly the oxygen reduction reaction (ORR). The lone pairs of electrons on pyridinic N can chemisorb O_2 molecules and facilitate their reduction. Bandgap Engineering: The larger covalent radius of S (1.04 Å) compared to C (0.77 Å) induces significant structural distortion and strain in the carbon lattice

when it substitutes a carbon atom (thiophene-S). This lattice strain leads to a narrowing of the bandgap, often resulting in longer-wavelength (red) emission, which is highly desirable for biomedical applications to reduce background autofluorescence and increase tissue penetration.

Enhanced redox activity: Sulfur-containing functional groups like sulfoxide (—S=O), sulfonic acid ($-SO_3H$), and thiol (—SH) on the CD surface can participate in reversible redox reactions. This makes S-doped CDs excellent for electrochemical sensing and as catalysts for oxidation reactions. The electron-donating capability of thiol/sulfide groups can also improve charge transfer.

4.3 Phosphorus doping

Phosphorus (P), which has a lower electronegativity, donates electrons and modifies carbon formation by creating Lewis basic sites on carbon, driven by changes in electronic energies. It introduces electron density into the carbon network by phosphonate/phosphate groups or lattice dopants (as C–P bonds) and creates electron-rich centers that function as adduct sites for Lewis acid species such as metal ions or electron-accepting gases. These features can improve the charge storage performance and ion-transport capability for supercapacitors and batteries. Phosphorus atom also creates defects promoting electrochemistry.

4.4 Boron doping

To achieve p-type semiconductor C-dots, boron (B) served as an electron acceptor owning to a lower electronegativity. Replacing a tetravalent carbon with a trivalent boron will form a “hole” structure in the valence band and endow B-doped C-dots as p-type materials which are necessary for p-n heterojunctions in optoelectronic devices. Boron species could be active sites for oxidants (H_2O_2 or molecular oxygen) activation and B-doped C-dot acted as efficient catalyst in the oxidation reaction. Heteroatom doping is a powerful approach for the functionalization of carbon dots (with different heteroatoms providing specific electronic features), more precisely, N increases electron density, S creates strain in the lattice and red-shifted emission, P induces Lewis basicity and improves electrochemical storage capacity, B introduces p-type character useful for optoelectronics and oxidative catalysis.

Furthermore, co-doping (e.g., N,S, N,P, B,N) has emerged as a superior strategy, where the synergistic effect between dopants can create even more pronounced modifications. For instance, N,S-co-doping can create a charge-polarized surface with N as the electron-accepting site and S as the electron-donating site, leading to unprecedented catalytic activity, as highlighted in works like Sun et al.,[99]. This level of control positions heteroatom doping as an indispensable methodology in the rational design of carbon dots for advanced technological applications.

5 Surface passivation of carbon dots

Boron surfactant passivation alleviates the surface defects introduced non-radiative recombination, leading to the enhanced PLQY and stability of C-dots[100]. Passivants are polymers, small molecules, and inorganic shells. Polymer films, such as polyacrylamide, increase emission by reducing vibrational energy loss. Low-molecular-weight passivating molecules, such as polyethyleneimine (PEI), endow optoelectronic controllability. Silica acts as shield for the core C-dots against quenchers, which leads to higher photostability and chemical stability. Advanced surface passivation of C-dots can open up its complete photophysics.

5.1 Hybridization and composite formation

CDs are ultrasmall, surface-functionalized carbon nanoparticles whose optical/electronic properties (strong, tunable photoluminescence, surface states, and facile surface chemistry) make them excellent photosensitizers, charge-transfer mediators, and surface-active co-catalysts when coupled to wide-bandgap semiconductors. Hybrid CD/semiconductor composites (TiO_2, ZnO, g-C_3N_4) typically show extended visible-light absorption, suppressed electron-hole recombination, and enhanced surface redox chemistry (higher ROS formation or H_2 evolution), provided the energy-level alignment and interfacial contact are optimized[101].

Fig. 6a(i) illustrates the dual functionality of CD/TiO_2 nanocomposites under solar light. In processes like water splitting and pollutant degradation, sunlight excites TiO_2, generating electrons and holes. The electrons reduce water to produce hydrogen gas (H_2), while the holes oxidize and break down pollutants into harmless CO_2 and water. The incorporated CDs play a crucial role by extending the composite's light absorption into the visible spectrum and acting as electron conduits, which enhances the overall efficiency. Fig. 6a(ii) illustrates an advanced application in organic synthesis. Here, the light-driven electron transfer between the CDs and TiO_2 is harnessed to activate a nickel-based catalyst. This activation enables cross-coupling reactions, where aryl halides (Ar—X) bond with various nucleophiles (Nu—H) to form new carbon-carbon (C—C) or carbon-heteroatom (C—X) bonds, yielding valuable coupled products (Ar—Nu).

Fig. 6b details the mechanism by which CQDs-modified ZnO degrades Rhodamine B (RhB) dye. Upon light exposure, ZnO absorbs energy, exciting electrons to its conduction band and leaving holes in its valence band. The CQDs, bonded to ZnO, act as efficient electron acceptors. This rapid electron transfer to the CQDs prevents the charges from recombining. The separated charges then drive the formation of reactive oxygen species: the electrons on the CQDs convert oxygen (O_2) into superoxide radicals ($\cdot O_2^-$), while the holes in ZnO oxidize water to generate hydroxyl radicals (·OH). These powerful radicals collaboratively attack and mineralize the RhB dye molecules. The CQDs thus boost performance by improving visible-light capture and sustaining charge separation.

Fig. 6c shows the wide application of a combination between g-C_3N_4 and CDs using composite. The synergy effects from g-C_3N_4 and CDs bring relatively unique light-adsorption, more effective charge separation, and greater surface activity. Overall, these data collectively demonstrate that the combination of the carbon dots with semiconductor photocatalysts (TiO_2, ZnO, g-C_3N_4) leads to versatile composites with enhanced efficiency and potential extensive applications in not only environmental remediation but also solar fuel production and organic synthesis.

In CD/TiO_2 composites, the wide bandgap of TiO_2 (3.2 eV), suffers from photocorrosion and electron hole recombination[105]. The addition of CDs sensitizes ZnO to visible light and protects it from photocorrosion by rapidly extracting photogenerated electrons and passivating the surface. Heteroatom-doped CDs (such as N- or S-doped) can also modulate the electronic structure of ZnO, inducing midgap states that broaden absorption and improve redox activity. Consequently, CDs/ZnO systems often exhibit superior degradation efficiency for organic pollutants and higher photocurrent density compared to pristine ZnO. CD/g-C_3N_4 composites are notable for their metal-free composition, narrow bandgap (~ 2.7 eV), and layered structure, making g-C_3N_4 an attractive photocatalyst for solar energy conversion[106–107]. However, pristine g-C_3N_4 suffers from low quantum efficiency and rapid carrier recombination. When hybridized with CDs, visible-light absorption increases, and overall charge separation efficiency improves. CDs can function as electron mediators in a direct Z-scheme system or participate in a Type-II heterojunction mechanism, depending on their energy-level alignment. Reports indicate that the photocatalytic activity of g-C_3N_4 can increase by more than tenfold with optimal incorporation of CDs, especially for hydrogen evolution and pollutant degradation. The formation of CD/semiconductor composites is a promising approach for efficient and stable environmental remediation and energy conversion applications. Key factors influencing photocatalytic performance include interfacial contact between CDs and semiconductor particles, optimal loading content, and controlled synthesis routes (hydrothermal, solvothermal, or in-situ growth). Although significant progress has been made, challenges remain in standardizing synthesis protocols, understanding charge-transfer pathways (Type-II vs. Z-scheme), and ensuring long-term stability for practical applications. Future research should incorporate time-resolved spectroscopy,

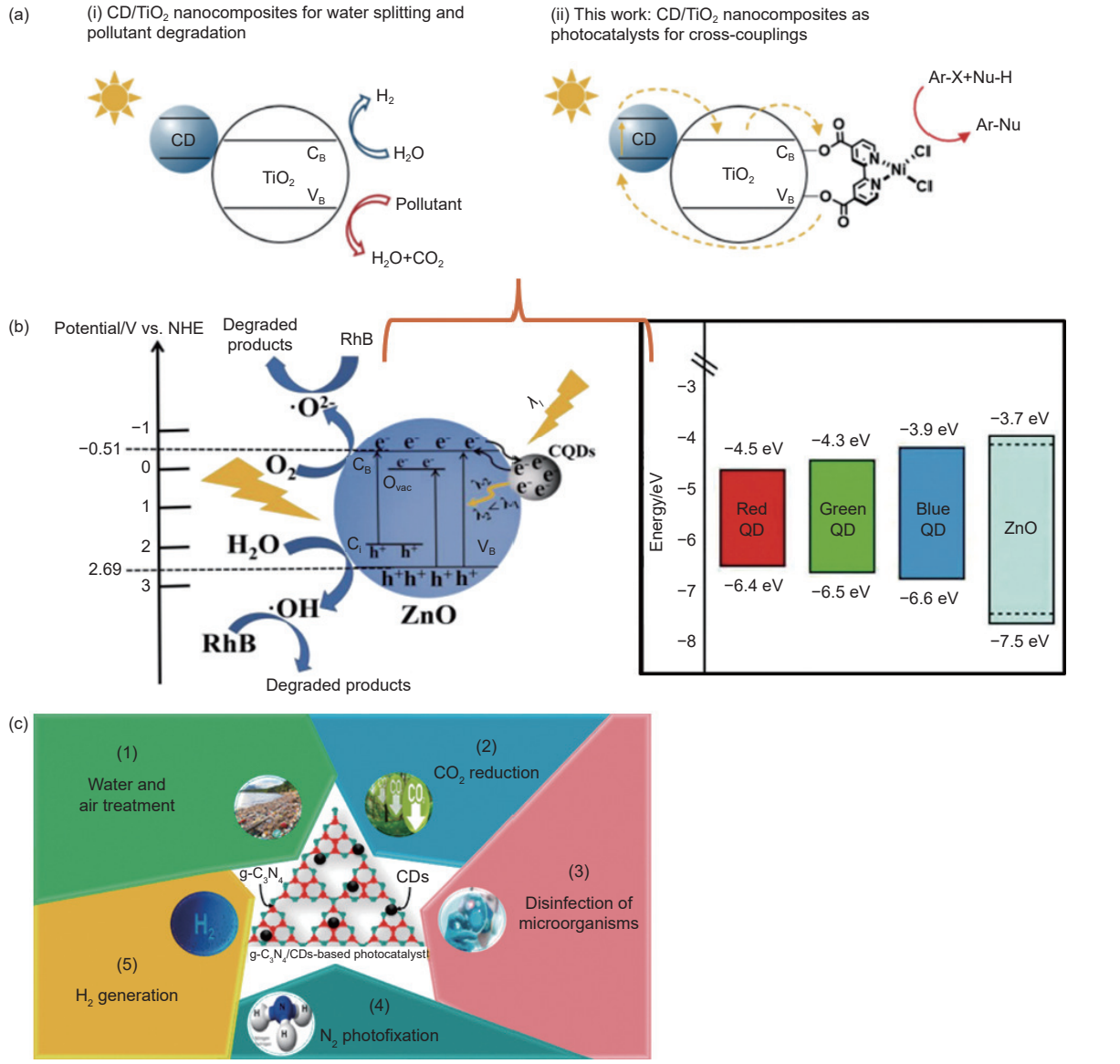

Fig. 6 (a) Schematic representation of CD/TiO_2 nanocomposites as (i) photocatalysts for water splitting, pollutant degradation and (ii) metallaphoto-catalytic carbon heteroatom cross-couplings[102]. Copyright 2021, Royal Chemistry Society. (b)Possible photodegradation mechanism of RhB over the CQDs/ZnO composite[103]. Copyright 2023, American Chemical Society. (c) Schematic representation of the multifunctional applications of g-C_3N_4/carbon dot (CDs)-based photocatalysts, including (1) water and air treatment, (2) CO_2 reduction, (3) disinfection of microorganisms, (4) N_2 photofixation, and (5) H_2 generation[104]. Copyright 2020, Elsevier

energy-level mapping, and life-cycle analysis to establish robust design principles for next-generation carbon-based hybrids[108].

6 Environmental remediation applications

Environmental pollution, particularly of water systems, is a critical global challenge due to the annual discharge of billions of tons of industrial and domestic waste[109]. CDs have recently emerged as highly promising nanomaterials for this purpose due to their superior properties, including broad-spectrum light absorption, upconversion luminescence, and excellent electron transfer capabilities[110]. Their straightforward synthesis, low energy requirements, and compatibility with solar energy make CDs a viable and attractive solution for environmental cleanup. This chapter details the fundamentals of CDs, their synthesis, the mechanisms of CDs-based photocatalysis, and their applications in environmental remediation[111].

CDs are metal-free, renewable photocatalysts used for decontaminating organic pollutants in wastewater. They provide tunable light absorption and good stability in water. CDs directly absorb photons and promote electrons to higher energy levels, generating charge pairs when illuminated by visible light. Their carbon-altered core can promote charge separation, preventing recombination. This results in a highly efficient production of oxidants such as hydroxyl and superoxide radicals which degrade contaminates[112]. Electrons drive dissolved oxygen reduction to superoxide radicals ($\bullet O_2^-$), and holes either oxidize water or hydroxyl groups giving origin to hydroxyl radicals (•OH). Oxygen radicals, such as superoxide, may be converted into hydrogen peroxide and further •OH radicals thereby achieving a synergistic action to degrade the pollutants to innocuous chemicals such as CO_2 and H_2O[113].

The attack by •OH and $\bullet O_2^-$ radicals targets the chromophoric center of the MB molecule, breaking the conjugated system responsible for its color and cleaving the heterocyclic rings. Similarly, rhodamine B (RhB), a xanthene dye, is degraded through N-deethylation, chromophore destruction, and ring-opening, all mediated by ROS generated from photoexcited CDs. Beyond dyes, CDs are effective against persistent and toxic pollutants like phenol. The degradation of phenol involves hydroxylation of the aromatic ring by •OH radicals, forming catechol, hydroquinone, and benzoquinone as intermediates, which are further oxidized and cleaved into aliphatic carboxylic acids before final mineralization to carbon dioxide and water[114]. The versatility of CDs in de grading a wide spectrum of pollutants underscores their potential as a robust, eco-friendly, and effective photocatalyst for advanced oxidation processes in environmental cleanup.

Fig. 7a shows the CDs/MIL-88B(Fe)/Bi_2S_3 heterojunction photocatalyst. The diagram uses an energy level diagram (with potentials in eV versus the normal hydrogen electrode, NHE) to show how the combination of three materials CDs, a metal-organic framework (MIL-88B(Fe)), and bismuth sulfide (Bi_2S_3) creates a system for efficient charge separation upon light absorption. Photogenerated electrons (e^-) in the Bi_2S_3 semiconductor are excited from the valence band (V_B, +0.91 eV) to the conduction band (C_B, −0.29 eV). These electrons then transfer to the CDs, which have a lowest unoccupied molecular orbital (LUMO) level at −0.2 eV, a suitable potential for reducing oxygen to generate reactive superoxide radicals. Simultaneously, the photogenerated holes (h^+) left in the V_B of Bi_2S_3 transfer to the highest occupied molecular orbital (HOMO) of MIL-88B(Fe) at +2.13 eV, which has a sufficiently positive potential to directly oxidize water or pollutants, with the pathway for generating hydroxyl radicals (•OH) also indicated. The proposed photocatalytic mechanism for hydrogen production (Fig. 7b) using the CdSQDs/Bi_2S_3 nanocomposite and Na_2SO_3/Na_2S sacrificial agents is illustrated in Fig. 6b. Under simulated solar light, both narrow-bandgap components are excited. Their inherent C_B and V_B positions are 0.11 eV/1.43 eV for Bi_2S_3 and −0.66 eV/1.72 eV for CdSQDs. However, the high photon energy of solar irradiation further elevates their excited-state potentials to approximately −1.53 and −1.31 eV, respectively.

7 Renewable energy applications of carbon dots

A particularly effective strategy for enhancing overall water splitting efficiency is the construction of Z-scheme photocatalytic systems, which mimic natural photosynthesis[117]. These systems facilitate superior charge separation and retain strong redox potentials, making them ideal for the simultaneous evolution of H_2 and O_2[118]. In contrast to conventional Type-II band alignment, a direct Z-scheme heterojunction is engineered to preserve the highest redox potentials of the constituent photocatalysts, thereby mimicking the essential charge transfer pathway of natural photosynthesis[119]. This configuration typically involves two semiconductors with staggered band positions like a Type-II system[120]. However, the charge migration mechanism is fundamentally different. Upon photoexcitation, instead of electrons and

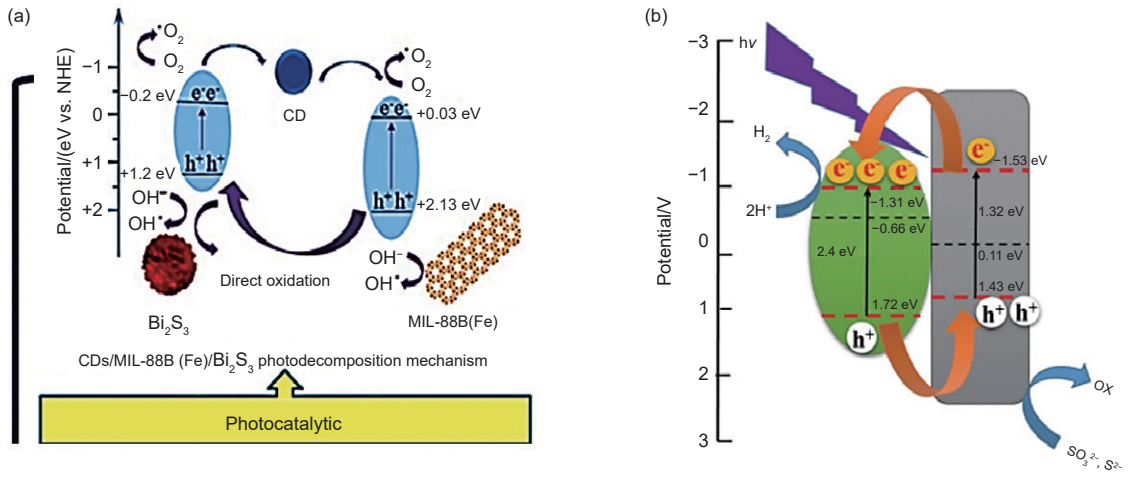

Fig. 7 (a) Possible photodecomposition mechanism for CDs/MIL-88B (Fe)/Bi2S3 nanocomposite under LED light[115]. Copyright 2021, Elsevier. (b) Plausible photocatalytic mechanism of CdSQDs/Bi_2S_3 nanocomposite[116]. Copyright 2019, Springer

holes migrating to the lowest C_B and highest V_B, respectively, a direct interfacial charge recombination occurs between the less useful charge carriers[121]. Specifically, the photogenerated electrons in the semiconductor with the lower (less negative) reduction potential readily recombine with the holes in the semiconductor with the lower (less positive) oxidation potential. This selective recombination pathway effectively quenches the low-energy charges while isolating the most energetically potent electrons in the higher CB and the most powerful holes in the higher VB. Consequently, the system maintains strong driving forces for both reduction and oxidation reactions simultaneously. This architecture is particularly advantageous for applications such as overall water splitting and CO_2 reduction, which demand both highly reductive electrons for proton or CO_2 reduction and highly oxidative holes for water oxidation. The CdS/Bi_2S_3 nanocomposite discussed herein exemplifies this principle, where the interface facilitates the recombination of Bi_2S_3 electrons with CdS holes, thereby preserving the highly negative photoexcited electrons in CdS for efficient hydrogen evolution[122].

7.1 CO_2 reduction

CDs are widely studied as photocatalysts, commonly for degrading organic molecules. However, their most significant potential lies in more complex reactions like CO_2 reduction and water splitting. The mechanism is attributed to the electrons released after light absorption. This is supported by experiments where adding noble metals to CDs captured these electrons, which quenched fluorescence but boosted CO_2 reduction efficiency. A key finding was that the yield of CO_2 reduction products surprisingly depends on the concentration of CO_2 itself. In the experiment, researchers adjusted CO_2 concentration by varying its pressure in a high-pressure optical cell containing an aqueous solution. They used gold-doped CDs as the visible-light photocatalyst and isopropanol as a sacrificial electron donor (Fig. 8).

7.2 Solar cells and DSSCs

C-dots can improve dye-sensitized solar cells (DSSCs) by sensitization or co-sensitization[124−125]. They are standalone sensitizers which can cover a broad range of UV-vis region and inject electron into the semiconductor oxides (NiO[124]/ZnO[126]/TiO_2[127]) upon excitation. As co-sensitizers to the conventional dyes, the C-dots can help energy injections by Förster Resonance Energy Transfer (FRET)[4], enhance spec-

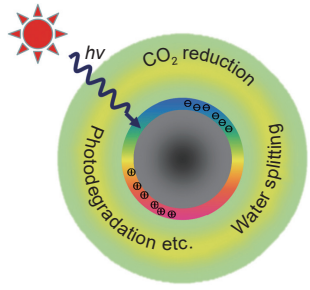

Fig. 8 Cartoon illustration of photocatalytic energy conversion applications of CDots[123]. Copyright 2019, AIP Publishing

tral response and reduce competitive absorption. They also facilitate charge separation, reduce recombination losses, and contribute to the light harvesting and charge transfer offers better PCE.

The schematic illustration in Fig. 9a below represents the charge transfer mechanism in a C-dot/N719/NiO-based dye-sensitized solar cell (DSSC). Upon visible-light irradiation, carbon dots (C-dots) act as photosensitizers, absorbing photons and exciting electrons from the highest occupied molecular orbital (HOMO) to the lowest unoccupied molecular orbital (LUMO). The excited electrons are subsequently injected into the C_B of NiO, facilitating charge separation and photocurrent generation. Meanwhile, holes remaining in the C-dots are transferred to the N719 dye, suppressing electron–hole recombination and enhancing charge transport efficiency. The red crosses indicate undesirable electron recombination pathways: (1) between injected electrons and oxidized species at the NiO/C-dot interface, (2) between electrons in C-dots and triiodide (I_3^-) ions, and (3) between the HOMO level of C-dots and I_3^- species in the electrolyte. The iodide/triiodide (I^-/I_3^-) redox couple serves to regenerate the oxidized dye molecules, closing the catalytic cycle. This synergistic interaction between C-dots, N719 dye, and NiO enhances light harvesting, promotes efficient charge separation, and minimizes recombination losses, leading to improved photovoltaic performance under visible light.

The schematic diagram in Fig. 9b illustrates the charge transfer and separation mechanism in a C-dot/N719/ZnO/NiO heterojunction-based photoelectrochemical cell under solar illumination. Upon visible-light irradiation, the C-dots and N719 dye serve as dual sensitizers, effectively harvesting photons and exciting electrons from their HOMO to LUMO energy levels. The excited electrons are injected sequentially from the LUMO of C-dots into the conduction band (C_B) of ZnO, and subsequently to the C_B of NiO, facilitating efficient charge transport toward the external circuit to generate photocurrent. Meanwhile, the photogenerated holes (h^+) in the HOMO of N719 are transferred to the valence band (V_B) of NiO, promot-

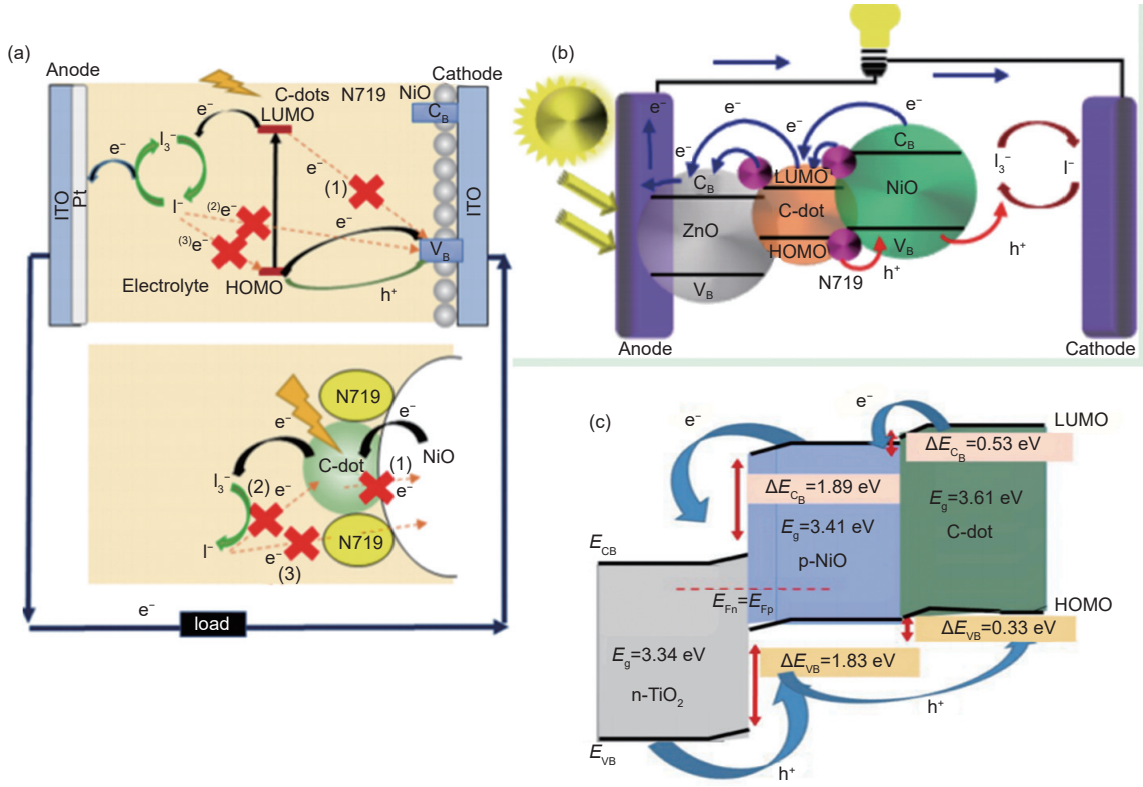

Fig. 9 DSSCs mechanism of Carbon dots with (a) NiO[124], Copyright 2020, American Chemical Society (b) ZnO[128]. Copyright 2020, American Chemical Society and (c) TiO_2[129], Copyright 2023, Elsevier

ing charge separation and suppressing recombination. The iodide/triiodide (I^-/I_3^-) redox couple in the electrolyte regenerates the oxidized dye and completes the catalytic cycle by transferring electrons back to the anode. The synergistic effect among ZnO, C-dots, NiO and N719 dye broadens the light absorption range, enhances interfacial charge transfer, and improves overall solar-to-electric conversion efficiency through effective suppression of electron-hole recombination pathways.

The schematic energy band diagram in Fig. 9c illustrates the charge transfer mechanism across the n-TiO_2/p-NiO/CD heterojunction, demonstrating efficient charge separation and transport under photoexcitation. The CDs, having a bandgap of 3.61 eV, act as visible-light sensitizers, facilitating electron excitation from the HOMO to the LUMO upon illumination. The photogenerated electrons in the LUMO of C-dots are transferred to the conduction band (E_{CB}) of p-NiO and subsequently to *n*-TiO_2, driven by the favorable conduction band offsets (ΔE_{CB} = 0.53 eV and 1.89 eV, respectively). Meanwhile, holes (h^+) migrate in the opposite direction from the valence band (E_{VB}) of TiO_2 to that of NiO and further to the HOMO of C-dots guided by the valence band offsets (ΔE_{VB} = 0.33 and 1.83 eV). This cascade-type band alignment effectively promotes directional charge migration, minimizes electron–hole recombination, and enhances the separation of photoinduced charge carriers. The matched Fermi levels ($E_{Fn} = E_{Fp}$) between TiO_2 and NiO establish a strong internal electric field at the interface, further supporting efficient charge transport, making this heterostructure highly favorable for applications in photocatalysis and solar energy conversion.

Carbon dots serve as excellent sensing platforms due to their tunable fluorescence, high sensitivity, and selective response to various analytes through mechanisms such as fluorescence quenching (static/dynamic), the inner filter effect, or fluorescence enhancement. As shown in Table 4, CDs demonstrate remarkable versatility and performance across multiple domains, as evidenced by their application in bioimaging, energy, photocatalysis, and antibacterial therapy. In bioimaging, CDs derived from natural precursors such as aloe vera, honey, and chitosan exhibit high quantum yields (up to 31.2%) and excellent photostability, enabling prolonged imaging in HeLa cells, zebrafish, and bacterial systems. For energy applications, CDs enhance device efficiency and longevity, achieving a power conversion efficiency of 8.7% in solar cells, a high specific capacity in lithium-ion batteries, and exceptional cyclic stability in fuel cells. In photocatalysis, they drive efficient degradation of pollutants (e.g., 98% methylene blue removal) and CO_2

Table 4 Application, stability/efficiency of C-dots

Cell/organism	Precursor	Quantum yield/%	Photostability	Ref.
Bioimaging applications of carbon dots				
HeLa cells	Aloe vera	24.6	>2 h continuous	[130]
MCF-7 cells	Honey	31.2	>90% intensity after 1 h	[131]
Zebrafish	Chitosan	19.8	3 h continuous	[132]
Bacterial cells	Tulsi leaves	22.1	Superior to FITC	[133]
Energy applications of carbon dots				
Solar cells	Garlic	PCE: 8.7%	500 h, 90% retention	[134]
Lithium-ion batteries	Grass	1250 mAh g^{-1} after 100 cycles	200 cycles, 85% capacity	[40]
Fuel cells	Chitosan	Onset potential: 0.91 V	10 000 cycles stable	[135]
Photocatalytic applications of carbon dots				
Methylene blue degradation	Banana peel	98% in 60 min	5 cycles, 90% efficiency	[136]
Cr(VI) to Cr(III) reduction	Grass	95% in 90 min	8 cycles stable	[137]
CO_2 reduction	Coffee grounds	84% conversion to CH_3OH	50 h stable	[138]
Antibacterial applications of carbon dots				
E. coli	Neem leaves	85% reduction	98% wound closure in 14 days	[139]
S. aureus	Banana peel	78% reduction	Complete healing in 10 days	[140]
MRSA	Garlic	92% reduction	2× faster than control	[141]

conversion with sustained activity over multiple cycles. Additionally, CDs display potent antibacterial effects against pathogens like *E. coli* and MRSA, promoting wound healing and demonstrating potential for therapeutic use. Their synthesis from renewable biomass, coupled with high efficiency, stability, and multifunctionality, positions CDs as promising sustainable nanomaterials for advanced technological and biomedical applications.

8 Conclusions, challenges and prospects

The origin and applications of biomass-assisted B-CDs are described in this review as being promising nanomaterials. Sustainable fabrication of tunable nanocarbons is summarizes. Eco-friendly synthesis methods, such as hydrothermal, pyrolysis, solvent and ultrasonic methods, allow the sustainable preparation of nanocarbons. The treatments improve the optical and electronic properties of B-CDs for different purposes. B-CDs are effective photocatalysts for pollutant degradation, possess antibacterial activity during wastewater treatment, and are widely used as photocatalysts in water splitting for hydrogen generation. They are good bio-imaging agents due to their biocompatibility and luminescence. Due to the versatility of B-CDs, tremendous applications have been realized such as in energy, environment and biomedical fields.

Although the synthesis has improved, challenges in scaling up C-dot technology remain[142−143]. The bottleneck is the diversity and incomparable natural precursors, which make it difficult to control the size, surface functionalization, and optical properties of B-CDs, hindering understanding of property relationships and large-scale reproducibility. B-CDs suffer from high charge recombination and poor visible light absorption, resulting in a relatively low hydrogen generation efficiency for photocatalytic water splitting than the inorganic counterpart[144]. Furthermore, the long-term photostability, reusability and environmental application of CDs in practice should be further explored[145]. The trend future should be from experience synthesis to design knowledge-based and package integration. Machine learning based "process structure property" studies will be indispensable for predicting the precursor-synthesis combination, which would yield the desired B-CDs with specific bandgap and surface states. Doping with heteroatoms (N, S, and P) or creating heterojunctions with semiconductors (g-C_3N_4, TiO_2) promote charge separation and photocatalytic activity for environmental purification or hydrogen production[146]. The development of scalable, continuous-flow synthesis approaches according to green chemistry is a prerequisite for homogeneity. In addition, researching the potential non-toxic multifunctional B-CD analogs in theranostics for photoimaging, antibacterial therapy and targeted drug delivery may contribute to personalized treatment because of their good biocompatibility[147].

The future lies in moving beyond empirical synthesis towards intelligent design and hybrid integration. Advanced "process structure property" studies, powered by machine learning, will be crucial for predicting optimal precursor-synthesis combinations to yield B-CDs with tailored bandgaps and surface states. Purposeful heteroatom doping (e.g., with N, S, P) and the construction of heterojunctions with other semiconductors (e.g., g-C_3N_4, TiO_2) are key strategies to enhance charge separation and boost photocatalytic activity for both environmental remediation and hydrogen generation[146]. For real-world impact, the focus must shift to scalable, continuous-flow synthesis processes that maintain green chemistry principles while ensuring homogeneity. Finally, the exploration of B-CDs as non-toxic, multifunctional agents in theranostics combining their bioimaging, antibacterial, and targeted drug delivery capabilities represents a vibrant frontier for personalized medicine, leveraging their unique biocompatibility derived from natural source[147].

Author contributions

Habtamu F Etefa contributed to the conceptualization, methodology, investigation, formal analysis, visualization, writing—original draft preparation, and

review and editing of the manuscript. Francis B. Dejene provided supervision, project administration, approval of the final version, financial support, and administrative assistance. All authors have read and approved the final version of the manuscript.

Conflicts of interest

The authors declare no conflict of interest.

Acknowledgements

The authors sincerely thank Walter Sisulu University (WSU) for the support provided throughout this work.

References

[1] Periasamy P, Mohanta Y K. Global energy crisis: Need for energy conversion and storage. In: Green Nanomaterials in Energy Conversion and Storage Applications[J]. Apple Academic Press, 2024: 45-73.

[2] Etefa H F, Tessema A A, Dejene F B. Carbon dots for future prospects: synthesis, characterizations and recent applications: a review (2019–2023)[J]. C, 2024, 10(3): 60.

[3] Singh A, Kafle S R, Sharma M, et al. Comprehensive review on multifaceted carbon dot nanocatalysts: Sources and energy applications[J]. Catalysts, 2023, 13(11): 1446.

[4] Qureshi Z A, Dabash H, Ponnamma D, et al. Carbon dots as versatile nanomaterials in sensing and imaging: Efficiency and beyond[J]. Heliyon, 2024, 10(11): e31634.

[5] Dhenadhayalan N, Lin K C, Saleh T A. Recent advances in functionalized carbon dots toward the design of efficient materials for sensing and catalysis applications[J]. Small, 2020, 16(1): 1905767.

[6] Khairol Anuar N K, Tan H L, Lim Y P, et al. A review on multifunctional carbon-dots synthesized from biomass waste: design/fabrication, characterization and applications[J]. Frontiers in energy research, 2021, 9: 626549

[7] Nemera D J, Etefa H F, Kumar V, et al. Hybridization of nickel oxide nanoparticles with carbon dots and its application for antibacterial activities[J]. Luminescence, 2022, 37(6): 965-970.

[8] Matyjasik W, Matus K, Długosz O, et al. Preparation of biomass waste-derived carbon dots by the thermal degradation process[J]. ACS omega, 2025, 10(22): 22529-22548.

[9] Kang C, Huang Y, Yang H, et al. A review of carbon dots produced from biomass wastes[J]. Nanomaterials, 2020, 10(11): 2316.

[10] Wu J, Chen T, Ge S, et al. Synthesis and applications of carbon quantum dots derived from biomass waste: A review[J]. Environmental Chemistry Letters, 2023, 21(6): 3393-3424.

[11] Wang Y, Chen Y, Zhao H, et al. Biomass-derived porous carbon with a good balance between high specific surface area and mesopore volume for supercapacitors[J]. Nanomaterials, 2022, 12(21): 3804.

[12] Chakraborty R, Vilya K, Pradhan M, et al. Recent advancement of biomass-derived porous carbon based materials for energy and environmental remediation applications[J]. Journal of Materials Chemistry A, 2022, 10(13): 6965-7005.

[13] Cao W Q, Wang Z Z, Wan X, et al. Multifunctional CuS/GO heterodimensional structure for microwave absorption, electromagnetic interference shielding, and energy storage device[J]. Advanced Composites and Hybrid Materials, 2024, 7(6): 187.

[14] Cai D, Zhong X, Xu L, et al. Biomass-derived carbon dots: synthesis, modification and application in batteries[J]. Chemical Science, 2025, 16(12): 4937-4970.

[15] Usman M, Cheng S. Recent trends and advancements in green synthesis of biomass-derived carbon dots[J]. Eng, 2024, 5(3): 2223-2263.

[16] Mohammed J, Hyuksu H, Milan M, et al. Novel interconnected hierarchical porous carbon derived from biomass for enhanced supercapacitor application[J]. Journal of Electroanalytical Chemistry, 2023, 935: 117355.

[17] Gemeda G F, Etefa H F, Hsieh C C, et al. Preparation of ZnO/NiO-loaded flexible cellulose nanofiber film electrodes and their application to dye-sensitized solar cells[J]. Carbohydrate Polymer Technologies and Applications, 2022, 3: 100213.

[18] Ma Z, Wang L, Wang Z, et al. Recent advances of plastic waste-derived carbon materials for energy storage, environmental remediation and organic synthesis applications[J]. ChemCatChem, 2024, 16(23): e202401072.

[19] Tamilselvan S N, Shanmugan S. Towards sustainable solar cells: unveiling the latest developments in bio-nano materials for enhanced DSSC efficiency[J]. Clean Energy, 2024, 8(3): 238-257.

[20] Korir B K, Kibet J K, Ngari S M. A review on the current status of dye-sensitized solar cells: toward sustainable energy[J]. Energy Science & Engineering, 2024, 12(8): 3188-3226.

[21] Etefa H F, Kumar V. Hybrid photocatalyst nanomaterials in solar cell applications. In: multifunctional hybrid semiconductor photocatalyst nanomaterials: Application on health, energy and environment[J]. Springer, 2023, 221-238.

[22] Jalalah M, Han H, Nayak A K, et al. Biomass-derived metal-free porous carbon electrocatalyst for efficient oxygen reduction reactions[J]. Journal of the Taiwan Institute of Chemical Engineers, 2023, 147: 104905

[23] Etefa H F, Nemera D J, Dejene F B. Green synthesis of nickel

oxide NPs incorporating carbon dots for antimicrobial activities[J]. ACS omega, 2023, 8(41): 38418-38425.

[24] Çeşme M, Eskalen H, Başkaya S K. Fluorescent carbon dots from vegetable and fruit wastes and their applications[J]. Fruits and Vegetable Wastes, 2022, 365-383.

[25] Gupta D, Priyadarshi R, Tammina S K, et al. Fruit processing wastes as sustainable sources to produce multifunctional carbon quantum dots for application in active food packaging[J]. Food and Bioprocess Technology, 2025, 18(3): 2145-2169.

[26] Tolou-Shikhzadeh-Yazdi S, Shakibapour N, Hosseini S, et al. High-efficient synthesis of carbon quantum dots from orange pericarp as fluorescence turn-on probes for Ca^{2+} and Zn^{2+} ion detection and their application in trypsin activity characterization[J]. Iranian Journal of Basic Medical Sciences, 2023, 26(2): 190.

[27] Etefa H F, Nemera D J, Etefa K T, et al. Evaluation of physicochemical properties of zinc oxide and indium-tin oxide nanoparticles for photocatalysis and biomedical activities[J]. Current Applied Physics, 2024, 67: 133-142.

[28] Tegegn D F, Etefa H F, Tucho B G, et al. Bio-derived carbon dots from black mulberry fruits: experimental synthesis and computational insights with ethylenediamine for photocatalytic degradation performance[J]. Physica Scripta, 2025, 100: 105908

[29] Kundu A, Maity B, Basu S. Orange pomace-derived fluorescent carbon quantum dots: detection of dual analytes in the nanomolar range[J]. ACS omega, 2023, 8(24): 22178-22189.

[30] Sahu S, Behera B, Maiti T K, et al. Simple one-step synthesis of highly luminescent carbon dots from orange juice: application as excellent bio-imaging agents[J]. Chemical communications, 2012, 48(70): 8835-8837.

[31] Osterloh F E. Inorganic nanostructures for photoelectrochemical and photocatalytic water splitting[J]. Chemical Society Reviews, 2013, 42(6): 2294-2320.

[32] Mittal A, Teotia M, Soni R, et al. Applications of eggshell and egg shell membrane as adsorbents: a review[J]. Journal of Molecular Liquids, 2016, 223: 376-387.

[33] Chauhan A, Zubair S, Sherwani A, et al. Aloe vera induced biomimetic assemblage of nucleobase into nanosized particles[J]. PloS one, 2012, 7(3): e32049.

[34] Costa A I, Barata P D, Moraes B, et al. Carbon dots from coffee grounds: synthesis, characterization, and detection of noxious nitroanilines[J]. Chemosensors, 2022, 10(3): 113.

[35] Ala M. Evaluation of garlic derived carbon dots for citocompatibility and radical scavenging: from structure to properties[J]. Politecnico di Torino, 2024, 6.

[36] Manigandan P, Shanmugam R. Green preparation of fluorescence carbon nanoparticles using honey and its biomedical applications-an in vitro study[J]. Journal of Drug Delivery Science and Technology, 2025, 108: 106919.

[37] Paveethra S, Manisekaran H, Sasidharan S. Medicinal plants derived green carbon dots: synthesis, characterization and their potential applications in cancer therapy[J]. Asian Pacific Journal of Cancer Prevention, 2024, 25(10): 3393.

[38] Landa S T, Bogireddy N R, Kaur I, et al. Heavy metal ion detection using green precursor derived carbon dots[J]. Iscience, 2022, 25(2): 103816

[39] Dong Y, Pang H, Ren S, et al. Etching single-wall carbon nanotubes into green and yellow single-layer graphene quantum dots[J]. Carbon, 2013, 64: 245-251.

[40] Lu X, Xie S, Yang H, et al. Photoelectrochemical hydrogen production from biomass derivatives and water[J]. Chemical Society Reviews, 2014, 43(22): 7581-7593.

[41] Atchudan R, Edison T I, Aseer K R, et al. Hydrothermal conversion of Magnolia liliiflora into nitrogen-doped carbon dots as an effective turn-off fluorescence sensing, multi-colour cell imaging and fluorescent ink[J]. Colloids and Surfaces B: Biointerfaces, 2018, 169: 321-328.

[42] Kasibabu B B, D'souza S L, Jha S, et al. Imaging of bacterial and fungal cells using fluorescent carbon dots prepared from carica papaya juice[J]. Journal of fluorescence, 2015, 25(4): 803-810.

[43] Keşir M K, Yılmaz M D. Potato peel carbon dots produced via fixed bed pyrolysis reactor decorated 1-D TiO_2 nanorods for rapid removal of methylene blue, Cr (VI), Escherichia coli, and Aspergillus niger[J]. Industrial Crops and Products, 2024, 220: 119244.

[44] Saini A, Nandi A, Das Gupta G, et al. Green synthesis of curcumin loaded carbon dots as a sustained drug delivery for anticancer therapy[J]. Current Pharmaceutical Design, 2025, 31(28): 2282-2289.

[45] Wazir A H, Khan Q, Ullah F, et al. Green synthesis of highly luminous lemon juice-based carbon dots for antimicrobial assessment and fingerprint detection[J]. International Journal of Materials Research, 2025, 116(2): 102-113.

[46] Pooja D, Singh L, Thakur A, et al. Green synthesis of glowing carbon dots from carica papaya waste pulp and their application as a label-freechemo probe for chromium detection in water[J]. Sensors and Actuators B: Chemical, 2019, 283: 363-372.

[47] Shahbaz Md, Umme Salma Md. Zafar Alam, et al. Fluorescent/ photoluminescent carbon dots as a sensor for the selective and sensitive detection of Fe^{3+}/Fe^{2+} metal ions. A review of the last decade[J]. Journal of Fluorescence, 2025, 35: 7451-7474.

[48] Crista D M, Esteves da Silva J C, Pinto da Silva L. Evaluation of different bottom-up routes for the fabrication of carbon dots[J]. Nanomaterials, 2020, 10(7): 1316.

[49] Ren J, Opoku H, Tang S, et al. Carbon dots: a review with focus on sustainability[J]. Advanced Science, 2024, 11(35): 2405472.

[50] Lim S Y, Shen W, Gao Z. Carbon quantum dots and their applications[J]. Chemical Society Reviews, 2015, 44(1): 362-381.

[51] Liu H, Ye T, Mao C. Fluorescent carbon nanoparticles derived from candle soot[J]. Angewandte chemie, 2007, 119(34): 6593-6595.

[52] Thara C R, Mathew B. Microwave synthesized N-doped carbon dots for dual mode detection of Hg (II) ion and degradation of

malachite green dye[J]. Talanta, 2024, 268: 125278.

[53] Jamshidi A, Hasan M M, Lee M T. Comparative study on engineering properties and energy efficiency of asphalt mixes incorporating fly ash and cement[J]. Construction and Building Materials, 2018, 168: 295-304.

[54] Da Rocha J G, Junior M S, Macuvele D P, et al. Uncovering engineering and mechanistic insights in green synthesis of carbon dots from rice husks[J]. Chemical Engineering Journal, 2025, 505: 159364.

[55] Bressi V, Balu A M, Iannazzo D, Espro C. Recent advances in the synthesis of carbon dots from renewable biomass by high-efficient hydrothermal and microwave green approaches[J]. Current Opinion in Green and Sustainable Chemistry, 2023, 40: 100742.

[56] Phukan K, Sarma RR, Dash S, et al. Carbon dot based nucleus targeted fluorescence imaging and detection of nuclear hydrogen peroxide in living cells[J]. Nanoscale Advances, 2022, 4(1): 138-149.

[57] Li H, Yan X, Kong D, et al. Recent advances in carbon dots for bioimaging applications[J]. Nanoscale Horizons, 2020, 5(2): 218-234.

[58] Etefa H F, Dejene F B. Applications of green carbon dots in personalized diagnostics for precision medicine[J]. International Journal of Molecular Sciences, 2025, 26(7): 2846.

[59] Yadav P K, Chandra S, Kumar V, et al. Carbon quantum dots: synthesis, structure, properties, and catalytic applications for organic synthesis[J]. Catalysts, 2023, 13(2): 422.

[60] Kanwal A, Bibi N, Hyder S, et al. Recent advances in green carbon dots (2015–2022): synthesis, metal ion sensing, and biological applications[J]. Journal of Nanotechnology, 2022, 13(1): 1068-1107.

[61] Aslam R, Qihui W, Ruozhou W, et al. Synthesis methodology of carbon dots: modern trends and enhancements[J]. ACS Symposium Series, 2024(1469): 95-120.

[62] Hasan M R, Saha N, Quaid T, et al. Formation of carbon quantum dots via hydrothermal carbonization: Investigate the effect of precursors[J]. Energies, 2021, 14(4): 986.

[63] Tshiamo B L, Jerry O A, Olaniyi A F. Carbon dot nanoparticles synthesized from horticultural extracts for postharvest shelf-life extension of fruits and vegetables[J]. Plants, 2025, 14(16): 2523

[64] Supajaruwong S, Porahong S, Wibowo A, et al. Scaling-up of carbon dots hydrothermal synthesis from sugars in a continuous flow microreactor system for biomedical application as in vitro antimicrobial drug nanocarrier[J]. Science and technology of advanced materials, 2023, 24(1): 2260298.

[65] Kong J, Wei Y, Zhou F, et al. Carbon quantum dots: properties, preparation, and applications[J]. Molecules, 2024, 29(9): 2002.

[66] Kaur I, Batra V, Bogireddy N K. Chemical-and green-precursor-derived carbon dots for photocatalytic degradation of dyes[J]. Iscience, 2024, 27(2): 108920.

[67] Horikoshi S, Schiffmann R F, Fukushima J, et al. Microwave chemical and materials processing[J]. Microwave Chemical and Materials Processing, 2018, 1: 33-45.

[68] Dąbrowska S, Chudoba T, Wojnarowicz J. Current trends in the development of microwave reactors for the synthesis of nanomaterials in laboratories and industries: a review[J]. Crystals, 2018, 8(10): 379.

[69] Paraknowitsch J P, Thomas A. Doping carbons beyond nitrogen: an overview of advanced heteroatom doped carbons with boron, sulphur and phosphorus for energy applications[J]. Energy & Environmental Science, 2013, 6(10): 2839-2855.

[70] Chen J, Yuan M, Cai W, et al. Constructing the frustrated Lewis pairs within N, S-codoped carbon to reveal the role of adjacent heteroatom sites for highly effective removal of heavy metal ions[J]. Chemical Engineering Journal, 2021, 422: 130153.

[71] Zhu Y J, Chen F. Microwave-assisted preparation of inorganic nanostructures in liquid phase[J]. Chemical reviews, 2014, 114(12): 6462-6555.

[72] De Medeiros T V, Manioudakis J, Noun F, et al. Microwave-assisted synthesis of carbon dots and their applications[J]. Journal of Materials Chemistry, C 2019, 7(24): 7175-7195.

[73] Wang Q, Zheng H, Long Y, et al. Microwave–hydrothermal synthesis of fluorescent carbon dots from graphite oxide. Carbon, 2011, 49(9): 3134-3140.

[74] Irene F B, Maria M H, Fernando H. Microwave-driven synthesis of iron-oxide nanoparticles for molecular imaging[J]. Molecules 2019, 24(7): 1224

[75] Chen F F, Zhu Y J. Highly Efficient rapid preparation of inorganic nanostructured materials by microwave heating[J], 2024, 141 - 251

[76] MP A, Pardhiya S, Rajamani P. Carbon dots: an excellent fluorescent probe for contaminant sensing and remediation[J]. Small, 2022, 18(15): 2105579.

[77] Walekar L, Dutta T, Kumar P, et al. Functionalized fluorescent nanomaterials for sensing pollutants in the environment: A critical review[J]. TrAC Trends in Analytical Chemistry, 2017, 97: 458-467

[78] Chen M, Ma J, Feng Y, et al. Advancing aqueous zinc-ion batteries with carbon dots: a comprehensive review[J]. EcoEnergy, 2025, 3(2): 254-295.

[79] Jayakumar A, Radoor S, Kim J T, et al. Carbon quantum dots from natural sources[S]. 2025, ISBN: 9781003437857

[80] Mathew M, Paroly S, Athiyanathil S. Biopolymer-based electrospun nanofiber membranes for smart food packaging applications: a review[J]. RSC advances, 2025, 15(27): 21742-21779.

[81] Fahad Halim A, Poinern G J, Fawcett D, et al. Biomass-derived carbon nanomaterials: Synthesis and applications in textile wastewater treatment, sensors, energy storage, and conversion technologies[J]. CleanMat, 2025, 2(1): 4-58.

[82] Zhu S, Meng Q, Wang L, et al. Highly photoluminescent carbon dots for multicolor patterning, sensors, and bioimaging[J]. Angewandte Chemie International Edition, 2013, 52(14).

[83] Jiang L, Ding H, Xu M, et al. UV–Vis–NIR full-range responsive carbon dots with large multiphoton absorption cross sections and

deep-red fluorescence at nucleoli and in vivo[J]. Small 2020, 16(19): 2000680

[84] Sun Y P, Zhou B, Lin Y, et al. Quantum-sized carbon dots for bright and colorful photoluminescence[J]. Journal of the American Chemical Society, 2006, 128(24): 7756-7757.

[85] Tetsuka H, Nagoya A, Fukusumi T, et al. Molecularly designed, nitrogen-functionalized graphene quantum dots for optoelectronic devices[J]. Advanced Materials (Deerfield Beach, Fla), 2016, 28(23): 4632-4638.

[86] Zhao W B, Liu K K, Song S Y, et al. Fluorescent nano-biomass dots: ultrasonic-assisted extraction and their application as nanoprobe for Fe3+ detection[J]. Nanoscale Research Letters, 2019, 14(1): 130.

[87] Yin Q, Wang M, Fang D, et al, Cl-doped deep eutectic solvents-based carbon dots as a selective fluorescent probe for determination of morphine in food[J]. RSC advances, 2021, 11(27): 16805-16813.

[88] Dehvari K, Liu K Y, Tseng P J, et al. Sonochemical-assisted green synthesis of nitrogen-doped carbon dots from crab shell as targeted nanoprobes for cell imaging[J]. Journal of the Taiwan Institute of Chemical Engineers, 2019, 95: 495-503.

[89] Wang N, Zheng A Q, Liu X, et al. Deep eutectic solvent-assisted preparation of nitrogen/chloride-doped carbon dots for intracellular biological sensing and live cell imaging[J]. ACS applied materials & interfaces, 2018, 10(9): 7901-7909.

[90] ReddyPrasad P, Naidoo E B. Ultrasonic synthesis of high fluorescent C-dots and modified with $CuWO_4$ nanocomposite for effective photocatalytic activity[J]. Journal of Molecular Structure, 2015, 1098: 146-152.

[91] Waseem Basha Z, Muniraj S, Senthil Kumar A. Neem biomass derived carbon quantum dots synthesized via one step ultra sonification method for ecofriendly methylene blue dye removal[J]. Scientific Reports, 2024, 14(1): 9706.

[92] Cao M, Zhao X, Gong X. Ionic liquid-assisted fast synthesis of carbon dots with strong fluorescence and their tunable multicolor emission[J]. Small, 2022, 18(11): 2106683.

[93] Yan Y, Manickam S, Lester E, et al. Synthesis of graphene oxide and graphene quantum dots from miscanthus via ultrasound-assisted mechano-chemical cracking method[J]. Ultrasonics Sonochemistry, 2021, 73: 105519.

[94] Wang M, Li C, Zhou M, et al. Natural deep eutectic solvent assisted synthesis and applications of chiral carbon dots[J]. Green Chemistry, 2022, 24(17): 6696-6706.

[95] Wang M, Kang X, Deng L, et al. Deep eutectic solvent assisted synthesis of carbon dots using sophora flavescens aiton modified with polyethyleneimine: Application in myricetin sensing and cell imaging[J]. Food Chemistry, 2021, 345: 128817.

[96] Zhao N, Song J, Zhao L. Metallic deep eutectic solvents-assisted synthesis of Cu, Cl-doped carbon dots as oxidase-like and peroxidase-like nanozyme for colorimetric assay of hydroquinone and H_2O_2[J]. Colloids and Surfaces A: Physicochemical and Engineering Aspects, 2022, 648: 129390.

[97] Chen J, Li Y, Lv K, et al. Cyclam-functionalized carbon dots sensor for sensitive and selective detection of copper (II) ion and sulfide anion in aqueous media and its imaging in live cells[J]. Sensors and Actuators B: Chemical, 2016, 224: 298-306.

[98] Yan F, Jiang Y, Sun X, et al. Surface modification and chemical functionalization of carbon dots: a review[J]. Microchimica Acta, 2018, 185(9): 424.

[99] Boyce J H, Eschenbrenner-Lux V, Porco Jr J A. Syntheses of (+)-30-epi-, (−)-6-epi-, (±)-6, 30-epi-13, 14-didehydroxyisogarcinol and (±)-6, 30-epi-garcimultiflorone A utilizing highly diastereoselective, lewis acid-controlled cyclizations[J]. Journal of the American Chemical Society, 2016, 138(44): 14789-14797.

[100] Mikhail M M, Ahmed H B, Abdallah A E, et al. Surface passivation of carbon dots for tunable biological performance[J]. Journal of Fluorescence, 2024, 1-18.

[101] Jung H, Sapner V S, Adhikari A, et al. Recent progress on carbon quantum dots based photocatalysis[J]. Frontiers in Chemistry, 2022, 10: 881495.

[102] Zhao Z, Reischauer S, Pieber B, et al. Carbon dot/TiO_2 nanocomposites as photocatalysts for metalphotocatalytic carbon–heteroatom cross-couplings[J]. Green Chemistry, 2021, 23(12): 4524-4530.

[103] Xu J J, Lu Y N, Tao F F, et al. ZnO nanoparticles modified by carbon quantum dots for the photocatalytic removal of synthetic pigment pollutants[J]. ACS omega, 2023, 8(8): 7845-7857.

[104] Asadzadeh-Khaneghah S, Habibi-Yangjeh A. g-C_3N_4/carbon dot-based nanocomposites serve as efficacious photocatalysts for environmental purification and energy generation: a review[J]. Journal of Cleaner Production, 2020, 276: 124319.

[105] Khan M M, Ansari S A, Pradhan D, et al. Band gap engineered TiO_2 nanoparticles for visible light induced photoelectrochemical and photocatalytic studies[J]. Journal of Materials Chemistry A, 2014, 2(3): 637-644.

[106] Tegenaw A B, Yimer A A, Beyene T T. Boosting the photocatalytic activity of ZnO-NPs through the incorporation of C-dot and preparation of nanocomposite materials[J]. Heliyon 2023, 9(10).

[107] Mahala C, Sharma M D, Basu M. Type-II heterostructure of ZnO and carbon dots demonstrates enhanced photoanodic performance in photoelectrochemical water splitting[J]. Inorganic Chemistry, 2020, 59(10): 6988-6999.

[108] Kumar S, Dhiman A, Sudhagar P, et al. ZnO-graphene quantum dots heterojunctions for natural sunlight-driven photocatalytic environmental remediation[J]. Applied Surface Science, 2018, 447: 802-815.

[109] Abidin Z Z, Pudza M Y, Issa M A. Sustainable applications of carbon dots-based composites as photocatalyst for environmental pollutants remediation. In: Novel Materials for Environmental Remediation Applications[J]. Elsevier, 2023, 555-577.

[110] Soni H, Bhattu M, Kaur M, et al. Recent advances in waste-derived carbon dots and their nanocomposites for environmental remediation and biological applications[J]. Environmental

Research, 2024, 251: 118560.

[111] Park S J, Yang H K. Ultra-fast synthesis of carbon dots using the wasted coffee residues for environmental remediation[J]. Current Applied Physics, 2022, 36: 9-15.

[112] Li H, He X, Liu Y, et al. One-step ultrasonic synthesis of water-soluble carbon nanoparticles with excellent photoluminescent properties[J]. Carbon, 2011, 49(2): 605-609

[113] Wang R, Lu K Q, Tang Z R, et al. Recent progress in carbon quantum dots: synthesis, properties and applications in photocatalysis.[J] Journal of Materials Chemistry A, 2017, 5(8): 3717-3734.

[114] Mondal S, Yucknovsky A, Akulov K, et al. Efficient photosensitizing capabilities and ultrafast carrier dynamics of doped carbon dots[J]. Journal of the American Chemical Society, 2019, 141(38): 15413-15422

[115] Khasevani S G, Shahsavari S, Gholami M. Green synthesis of ternary carbon dots (CDs)/MIL-88B (Fe)/Bi_2S_3 nanocomposite via MOF templating as a reusable heterogeneous nanocatalyst and nano-photocatalyst[J]. Materials Research Bulletin, 2021, 138: 111204.

[116] Vattikuti S P, Nagajyothi P, Shim J. Fabrication of CdS quantum dot/Bi_2S_3 nanocomposite photocatalysts for enhanced H_2 production under simulated solar light[J]. Journal of Materials Science: Materials in Electronics, 2019, 30(6): 5681-5690.

[117] Abdul Nasir J, Munir A, Ahmad N, et al. Photocatalytic Z-scheme overall water splitting: recent advances in theory and experiments. Advanced Materials, 2021, 33(52): 2105195.

[118] Sun X, Yang J, Zeng X, et al. Pairing oxygen reduction and water oxidation for dual-pathway H_2O_2 production[J]. Angewandte Chemie International Edition, 2024, 63(52): e202414417.

[119] Zhang Z, Wang L, Chen D, et al. Recent developments in and perspectives on $ReFeO_3$-based composites for emerging photocatalytic applications: a critical review[J]. Catalysis Science & Technology, 2025, 15: 2406

[120] Lo SS, Mirkovic T, Chuang CH, et al. Emergent properties resulting from type-II band alignment in semiconductor nanoheterostructures[J]. Advanced Materials, 2011, 23(2): 180-197.

[121] Zhang P, Wang T, Chang X, et al. Effective charge carrier utilization in photocatalytic conversions. Accounts of chemical research, 2016, 49(5): 911-921.

[122] Shi J, Fan Y, Zhang Q, et al. Harnessing photo-energy conversion in nanomaterials for precision[J] Advanced Materials, 2025, 2501623.

[123] Cao L, Shiral Fernando K, Liang W, et al. Carbon dots for energy conversion applications[J]. Journal of Applied Physics, 2019, 125(22).

[124] Etefa H F, Imae T, Yanagida M. Enhanced photosensitization by carbon dots Co-adsorbing with dye on p-type semiconductor (Nickel Oxide) solar cells[J]. ACS applied materials & interfaces, 2020, 12(16): 18596-18608.

[125] Narayanan R. Charge transport processes in quantum dot sensitized solar cells[C]. Indian Institute of Technology, Hyderabad, 2014, Thesis.

[126] Manna A S, Ghosh S, Ghosh T, et al. Smart luminescent materials for emerging sensors: Fundamentals and advances[J]. Chemistry–An Asian Journal 2025, 20(6): e202401328.

[127] Kuvarega A T, Mamba B B. TiO_2-based photocatalysis: toward visible light-responsive photocatalysts through doping and fabrication of carbon-based nanocomposites[J]. Critical Reviews in Solid State and Materials Sciences, 2017, 42(4): 295-346

[128] Geleta T A, Imae T. Nanocomposite photoanodes consisting of p-NiO/n-ZnO heterojunction and carbon quantum dot additive for dye-sensitized solar cells[J]. ACS Applied Nano Materials, 2021, 4(1): 236-249.

[129] Yadeta T F, Imae T. Effect of carbon dot on photovoltaic performance of n-TiO_2/p-NiO and n-TiO_2/p-CuO heterojunctions in dye-sensitized solar cells[J]. Applied Surface Science, 2023, 637: 157880.

[130] Brouzgou A, Gorbova E, Wang Y, et al. Nitrogen-doped 3D hierarchical ordered mesoporous carbon supported palladium electrocatalyst for the simultaneous detection of ascorbic acid, dopamine, and glucose[J]. Ionics, 2019, 25(12): 6061-6070.

[131] Yang Z, Xu M, Liu Y, et al. Nitrogen-doped, carbon-rich, highly photoluminescent carbon dots from ammonium citrate[J]. Nanoscale, 2014, 6(3): 1890-1895.

[132] Yu L, Li X, He M, et al. Antioxidant carboxymethyl chitosan carbon dots with calcium doping achieve ultra-low calcium concentration for iron-induced osteoporosis treatment by effectively enhancing calcium bioavailability in zebrafish[J]. Antioxidants, 2023, 12(3): 583.

[133] Kumar V B, Tang J, Lee K J, et al. In situ sonochemical synthesis of luminescent Sn@ C-dots and a hybrid Sn@ C-dots@ Sn anode for lithium-ion batteries[J]. RSC advances, 2016, 6(70): 66256-66265.

[134] Sawires E F, Ismail Z, Samir M, et al. Exploring various integration methods of carbon quantum dots in $CsPbCl_3$ perovskite solar cells for enhanced power conversion efficiency[J]. Journal of Materials Science: Materials in Electronics, 2024, 35(11): 800.

[135] Wu Q, ang L, Yan Y, Li S, et al. Chitosan-derived carbon dots with room-temperature phosphorescence and energy storage enhancement properties[J]. ACS sustainable chemistry & engineering, 2022, 10(9): 3027-3036.

[136] Atchudan R, Edison T I, Perumal S, et al. Hydrophilic nitrogen-doped carbon dots from biowaste using dwarf banana peel for environmental and biological applications[J]. Fuel, 2020, 275: 117821.

[137] Gunture, Lee T Y. Biomass-derived multiatom-doped carbon dots for the photocatalytic reduction of Cr (VI) and precipitation of Cr (III)[J]. npj Clean Water, 2024, 7(1): 132.

[138] Muangmora R, Rojviroon O, Kemacheevakul P, et al. Spent coffee ground-derived carbon quantum dot composite with metal oxides for photocatalytic degradation of carbaryl in water and antibacterial application[J]. Journal of Water Process

Engineering, 2025, 70: 107145.

[139] Hunashyal A A, Masti S P, Kurabetta L K, et al. Neem leaf-derived carbon dot-embedded chitosan-based active films: a sustainable approach to prolong the shelf life of prawns[J]. Sustainable Food Technology, 2025, 3(6): 2088-2107.

[140] Meng Y, Zhu H, Li X, Zhao S, et al. Antimicrobial activity of carbon dots against aquatic spoilage Bacteria synthesized from Banana Peel waste[J]. Food Chemistry, 2025, 27: 102375.

[141] Wang Z, Sheng L, Yang X, et al. Natural biomass-derived carbon dots as potent antimicrobial agents against multidrug-resistant bacteria and their biofilms[J]. Sustainable Materials and Technologies, 2023, 36: e00584.

[142] Gao J, Zhu M, Huang H, et al. Advances, challenges and promises of carbon dots[J]. Inorganic Chemistry Frontiers, 2017, 4(12): 1963-1986.

[143] Tian X T, Yin X B. Carbon dots, unconventional preparation strategies, and applications beyond photoluminescence[J]. Small, 2019, 15(48): 1901803.

[144] Wang B, Waterhouse G I, Lu S. Carbon dots: mysterious past, vibrant present, and expansive future[J]. Trends in Chemistry, 2023, 5(1): 76-87.

[145] Wareing T C, Gentile P, Phan A N. Biomass-based carbon dots: current development and future perspectives[J]. ACS nano, 2021, 15(10): 15471-15501

[146] Mohapatra L, Patra D, Zaidi S, et al. Heterointerface engineered and highly dual-functional N-doped carbon dot/N-rich g-C_3N_4 hybrid photocatalysts[J]. Materials Today Chemistry, 2022, 26: 101081.

[147] Basavaraj N, Sekar A, Yadav R. Review on green carbon dot-based materials for the photocatalytic degradation of dyes: fundamentals and future perspective[J]. Materials Advances, 2021, 2(23): 7559-7582.